Models of Ciliary Dynamics

Charlotte Cook, Maitreya Das, Siddharth Mani, Kristina Newton

June 2026

Contents

1 Introduction

Cilia are short hair-like organelles on membranes. They are omnipresent in eukaryotes, from ciliates to various organ systems. Cilia are subdivided into motile and non-motile types. Carpets of motile cilia spontaneously form a beating pattern which helps propel micro-organisms and sweep mucus in the lungs [2].

Cilia beats are shaped by local and nonlocal forces. Locally, cilia motion is based on the sliding of doublet micro-tubules. Dynein arms connect adjacent micro-tubules and "walk" between them. This "walking" requires the use of ATP and Ca^{2+} ions and causes the micro-tubules to slide. [5] Hydrodynamic coupling and efficiency considerations generate the spontaneous metachronal coordination of cilia carpets necessary for normal physiological functioning. [4] These nonlocal forces are modeled with the Stokes equation in the low Reynolds number regime. The Reynolds number is a dimensionless parameter given by $Re = \frac{\rho U L}{\mu}$, where ρ is the fluid density, U is the characteristic velocity, L is the characteristic length, and μ is the dynamic viscosity of the fluid. The dimensionless Stokes equation in this case is given by the below equations.

$$\mathrm{Re}\left(\boldsymbol{u}_t + \boldsymbol{u} \cdot \nabla \boldsymbol{u}\right) = -\nabla p + \Delta \boldsymbol{u}$$
$$\nabla \cdot \boldsymbol{u} = 0$$

Additionally, a wall is imposed based on the image system for the method of regularized Stokeslets. [1]

We are primarily interested in generalizing De Canio et al's 2-Link Model [3] to explore these features of cilia beats. Briefly, the 2-Link Model comprises of two rigid links of length l joined together at point A (Figure 1). Elasticity is introduced by introducing two torsional springs with spring constant k. Our work includes deriving the N-link Model and three dimensional 2-Link Model, simulating beating patterns of multiple 2-Link Model cilia through hydrodynamic forces, and investigating the 2-Link Coupled Follower Model for dynein motion.

2 2-link Model

The following model was introduced by De Canio et al. in their 2017 paper, *Spontaneous oscillations of elastic filaments induced by molecular motors* [3]. The two-link model simplifies analysis of the dynamics by reducing the continuous filament into a discrete one with two beads, A and B.

2.1 Derivation

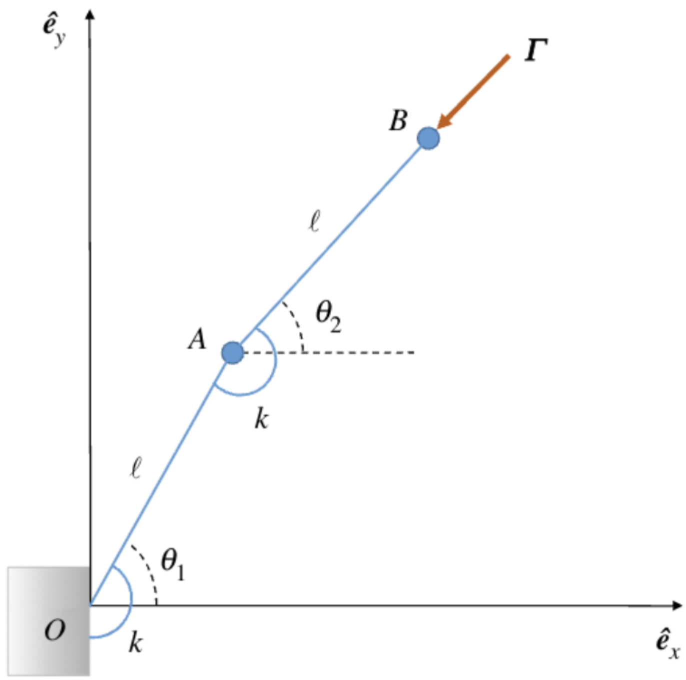

Figure 1: Two filament model from De Canio et al.

The angles of each hinge in figure 1 give the equations of motion with respect to the horizontal, θ_1 and θ_2. To derive the system of differential equations that describes the dynamics of the system, we first start with the vector-valued functions describing the positions of A and B, $\boldsymbol{r}_A$ and $\boldsymbol{r}_B$:

$$\boldsymbol{r}_A = A - O = l(\cos\theta_1, \sin\theta_1), \boldsymbol{r}_B = B - O = l(\cos\theta_1 + \cos\theta_2, \sin\theta_1 + \sin\theta_2).$$

Differentiating with respect to time gives us the velocities of A and B:

$$\begin{aligned}
\boldsymbol{v}_A = \dot{\boldsymbol{r}}_A &= \frac{d}{dt} l(\cos\theta_1, \sin\theta_1) \\
&= l(-\dot{\theta}_1 \sin\theta_1, \dot{\theta}_1 \cos\theta_1) = \dot{\theta}_1 l(-\sin\theta_1, \cos\theta_1) \\
\boldsymbol{v}_B = \dot{\boldsymbol{r}}_B &= \frac{d}{dt} l(\cos\theta_1 + \cos\theta_2, \sin\theta_1 + \sin\theta_2) \\
&= l(-\dot{\theta}_1 \sin\theta_1 - \dot{\theta}_2 \sin\theta_2, \dot{\theta}_1 \cos\theta_1 + \dot{\theta}_2 \cos\theta_2) \\
&= l[\dot{\theta}_1(-\sin\theta_1, \cos\theta_1) + \dot{\theta}_2(-\sin\theta_2, \cos\theta_2)].
\end{aligned}$$

Recall the *principle of virtual work*, which states that if a mechanical system in equilibrium undergoes an arbitrary, infintessimal change in displacement, the net "virtual" work done by all external forces in the system is 0. In the case of the two-link model, the net forces in question are:

1. the tangential force $\boldsymbol{\Gamma}$ applied at the tip of the second rod.
2. the fluid drag forces $\boldsymbol{F}_A$ and $\boldsymbol{F}_B$ applied to beads A and B.
3. the torsion spring forces F_{spr_O} and F_{spr_A} on O and A.

These forces can be calculated as follows:

<u>$\boldsymbol{\Gamma}$:</u> we have that $\boldsymbol{\Gamma} = \Gamma\hat{\boldsymbol{t}}$, where $\Gamma > 0$ is the magnitude of the force and $\hat{\boldsymbol{t}} = (\cos\theta_2, \sin\theta_2)$ is the unit vector centered at B.

<u>$\boldsymbol{F}_{A/B}$</u>: at small scales, the fluid drag force on an object is proportional to its velocity rather than its velocity squared. Thus, for effective constant ζ we have that $\boldsymbol{F}_A = -\zeta\boldsymbol{v}_A$ and $\boldsymbol{F}_B = -\zeta\boldsymbol{v}_B$.

<u>$F_{spr_{O/A}}$</u>: assuming the torsional springs at O and A have spring constant k, the restorative spring forces are then given by $F_{spr_O} = -k\theta_1$ and $F_{spr_A} = -k(\theta_2 - \theta_1)$.

- Note that the tension on A due to the second filament bending is relative to the amount the first filament bends; hence the force is proportional to $\theta_2 - \theta_1$ rather than just θ_2.

Now, applying the principle of virtual work, we can set the net virtual work to 0 (here $\delta(\cdot)$ represents an arbitrarily small change in $(\cdot)$, i.e. virtual displacements):

$$\boldsymbol{\Gamma}\delta\boldsymbol{r}_B + \boldsymbol{F}_A\delta\boldsymbol{r}_A + \boldsymbol{F}_B\delta\boldsymbol{r}_B + F_{spr_O}\delta\theta_1 + F_{spr_A}\delta(\theta_2 - \theta_1) = 0.$$

To simplify the derivation of the equations of motion from the virtual work equation, we will expand each term individually and gather terms as coefficients of $\delta\theta_1$ and $\delta\theta_2$. We do this in order to subsequently invoke the arbitrariness of $\delta\theta_1$ and $\delta\theta_2$, and thus set them equal to 0. First, it is helpful to expand the variations of $\boldsymbol{r}_A$ and $\boldsymbol{r}_B$:

$$\begin{aligned}
\delta\boldsymbol{r}_A &= \delta[l(\cos\theta_1, \sin\theta_1)] \\
&= \delta\theta_1 l(-\sin\theta_1, \cos\theta_1). \\
\delta\boldsymbol{r}_B &= \delta[l(\cos\theta_1 + \cos\theta_2, \sin\theta_1 + \sin\theta_2)] \\
&= \delta[l(\cos\theta_1, \sin\theta_1) + l(\cos\theta_2, \sin\theta_2)] \\
&= l[\delta\theta_1(-\sin\theta_1, \cos\theta_1) + \delta\theta_2(-\sin\theta_2, \cos\theta_2)].
\end{aligned}$$

<u>$\boldsymbol{\Gamma}\delta\boldsymbol{r}_B$:</u>

$$\begin{aligned}
\boldsymbol{\Gamma}\delta\boldsymbol{r}_B &= -\Gamma(\cos\theta_2, \sin\theta_2)\cdot l[\delta\theta_1(-\sin\theta_1, \cos\theta_1) + \delta\theta_2(-\sin\theta_2, \cos\theta_2)] \\
&= -\Gamma l[\delta\theta_1\underbrace{(-\sin\theta_1\cos\theta_2 + \sin\theta_2\cos\theta_1)}_{=\sin(\theta_2-\theta_1)} + \underbrace{\delta\theta_2(-\sin\theta_2\cos\theta_2 + \cos\theta_2\sin\theta_2)}_{=0}] \\
&= \delta\theta_1(-\Gamma l\sin(\theta_2 - \theta_1)) \\
&= \delta\theta_1(\Gamma l\sin(\theta_1 - \theta_2)).
\end{aligned}$$

<u>$\boldsymbol{F}_A\delta\boldsymbol{r}_A$:</u>

$$\begin{aligned}
\boldsymbol{F}_A\delta\boldsymbol{r}_A &= -\zeta l\dot{\theta}_1(-\sin\theta_1, \cos\theta_1)\cdot\delta\theta_1 l(\cos\theta_1, \sin\theta_2) \\
&= -\zeta l^2\dot{\theta}_1\delta\theta_1\underbrace{(\sin^2\theta_1 + \cos^2\theta_1)}_{=1} \\
&= \delta\theta_1(-\zeta l^2\dot{\theta}_1)
\end{aligned}$$

<u>$\boldsymbol{F}_B\delta\boldsymbol{r}_B$:</u>

$$
\begin{aligned}
\boldsymbol{F}_B \delta \boldsymbol{r}_B &= -\zeta l[\dot{\theta}_1(-\sin\theta_1, \cos\theta_1) + \dot{\theta}_2(-\sin\theta_2, \cos\theta_2)] \cdot l[\delta\theta_1(-\sin\theta_1, \cos\theta_1) + \delta\theta_2(-\sin\theta_2, \cos\theta_2)] \\
&= -\zeta l^2[\dot{\theta}_1 \delta\theta_1 (\underbrace{\sin^2\theta_1 + \cos^2\theta_1}_{=1}) + \delta\theta_1 \dot{\theta}_2 (\underbrace{\sin\theta_1 \sin\theta_2 + \cos\theta_1 \cos\theta_2}_{=\cos(\theta_1-\theta_2)}) + \\
&\quad \dot{\theta}_1 \delta\theta_2 (\underbrace{\sin\theta_1 \sin\theta_2 + \cos\theta_1 \cos\theta_2}_{=\cos(\theta_1-\theta_2)}) + \dot{\theta}_2 \delta\theta_2 (\underbrace{\sin^2\theta_2 + \cos^2\theta_2}_{=1})] \\
&= \delta\theta_1[-\zeta l^2(\dot{\theta}_2 \cos(\theta_1 - \theta_2) + \dot{\theta}_1)] + \delta\theta_2[-\zeta l^2(\dot{\theta}_1 \cos(\theta_1 - \theta_2) + \dot{\theta}_2)].
\end{aligned}
$$

$\underline{F_{spr_O}\delta\theta_1}$:

$$
F_{spr_O}\delta\theta_1 = (-k\theta_1)\delta\theta_1.
$$

$\underline{F_{spr_A}(\delta\theta_2 - \delta\theta_1)}$:

$$
\begin{aligned}
F_{spr_A}(\delta\theta_2 - \delta\theta_1) &= -k(\theta_2 - \theta_1)(\delta\theta_2 - \delta\theta_1) \\
&= \delta\theta_1[k(\theta_2 - \theta_1)] + \delta\theta_2[k(\theta_1 - \theta_2)].
\end{aligned}
$$

Thus, the virtual work equation expands to

$$
\underbrace{\left[\Gamma l \sin(\theta_1 - \theta_2) - \zeta l^2 \dot{\theta}_1 - \zeta l^2(\dot{\theta}_2 \cos(\theta_1 - \theta_2) + \dot{\theta}_1) - k l^2 \theta_1\right] \delta\theta_1}_{=C_1} + \underbrace{\left[-\zeta l^2(\dot{\theta}_1 \cos(\theta_1 - \theta_2) + \dot{\theta}_2) + k(\theta_1 - \theta_2)\right]}_{=C_2} \delta\theta_2 = 0
$$

Now we invoke the arbitrariness of $\delta\theta_1$ and $\delta\theta_2$; since they are independent and arbitrary, the only way for $C_1\delta\theta_1 + C_2\delta\theta_2 = 0$ to be true for any possible $\delta\theta_1$ and $\delta\theta_2$ is if C_1 and C_2 both equal 0. This gives us our system of ODEs as presented in [3] (equations 4.6 and 4.7 respectively). In order to simplify our equations, we non-dimensionalize it by rescaling the time variable as $\tilde{t} = \frac{k}{\zeta l^2} t \iff d\tilde{t} = \frac{k}{\zeta l^2} dt \iff dt = \frac{\zeta l^2}{k} d\tilde{t}$, which implies $\dot{\theta} = \frac{d\theta}{dt} = \frac{k}{\zeta l^2}\frac{d\theta}{d\tilde{t}} = \frac{k}{\zeta l^2}\theta'$. We also introduce a dimensionless forcing parameter $\Sigma = \frac{\Gamma l}{k}$:

<u>**Eq 4.6 in [3]** ($C_1 = 0$):</u>

$$
\begin{aligned}
\Gamma l \sin(\theta_1 - \theta_2) - \zeta l^2 \dot{\theta}_1 - \zeta l^2(\dot{\theta}_2 \cos(\theta_1 - \theta_2) + \dot{\theta}_1) - k\theta_1 + k(\theta_2 - \theta_1) &= 0 \\
\frac{\Gamma l}{k} \sin(\theta_1 - \theta_2) - \frac{\zeta l^2}{k}\dot{\theta}_1 - \frac{\zeta l^2}{k}(\dot{\theta}_2 \cos(\theta_1 - \theta_2) + \dot{\theta}_1) - 2\theta_1 + \theta_2 &= 0 \\
\Sigma \sin(\theta_1 - \theta_2) - \theta_1' - (\theta_2' \cos(\theta_1 - \theta_2) + \theta_1') - 2\theta_1 + \theta_2 &= 0 \\
\iff \boxed{\Sigma \sin(\theta_1 - \theta_2) - (\theta_2' \cos(\theta_1 - \theta_2) + 2\theta_1') - 2\theta_1 + \theta_2 = 0}
\end{aligned}
$$

<u>**Eq 4.7 in [3]** ($C_2 = 0$):</u>

$$
\begin{aligned}
-\zeta l^2(\dot{\theta}_1 \cos(\theta_1 - \theta_2) + \dot{\theta}_2) + k(\theta_1 - \theta_2) &= 0 \\
\frac{-\zeta l^2}{k}(\dot{\theta}_1 \cos(\theta_1 - \theta_2) + \dot{\theta}_2) + \theta_1 - \theta_2 &= 0 \\
\iff \boxed{-\theta_1' \cos(\theta_1 - \theta_2) - \theta_2' + \theta_1 - \theta_2 = 0}
\end{aligned}
$$

2.2 Linear Stability Analysis

To capture the transitions in this system, we linearize the equations of motion about the equilibrium configuration $\theta_1 = \theta_2 = 0$.

Step 1:

Applying the Taylor series approximations $\sin(x) \approx x$ and $\cos(x) \approx 1$,
Equation 4.6 in [3] simplifies:

$$\begin{aligned} \Sigma \sin(\theta_1 - \theta_2) - [2\dot{\theta}_1 + \dot{\theta}_2 \cos(\theta_1 - \theta_2)] - 2\theta_1 + \theta_2 &= 0 \\ \Sigma(\theta_1 - \theta_2) - [2\dot{\theta}_1 + \dot{\theta}_2(1)] - 2\theta_1 + \theta_2 &= 0 \\ \Sigma(\theta_1 - \theta_2) - 2\dot{\theta}_1 - \dot{\theta}_2 - 2\theta_1 + \theta_2 &= 0. \end{aligned}$$

Equation 4.7 in [3] simplifies:

$$\begin{aligned} -\dot{\theta}_1 \cos(\theta_1 - \theta_2) - \dot{\theta}_2 + \theta_1 - \theta_2 &= 0 \\ -\dot{\theta}_1(1) - \dot{\theta}_2 + \theta_1 - \theta_2 &= 0 \\ -\dot{\theta}_1 - \dot{\theta}_2 + \theta_1 - \theta_2 &= 0. \end{aligned}$$

Step 2:

Assume solutions of the form $\theta_j = \hat{\theta}_j e^{\omega \tilde{t}}$. Taking the derivative with respect to time yields $\dot{\theta}_j = \omega \hat{\theta}_j e^{\omega \tilde{t}}$. Substituting this into our linearized equations 4.6 and 4.7, we get equations 4.9 and 4.10 in [3].

$$\begin{aligned} \Sigma(\hat{\theta}_1 e^{\omega \tilde{t}} - \hat{\theta}_2 e^{\omega \tilde{t}}) - 2\omega\hat{\theta}_1 e^{\omega \tilde{t}} - \omega\hat{\theta}_2 e^{\omega \tilde{t}} - 2\hat{\theta}_1 e^{\omega \tilde{t}} + \hat{\theta}_2 e^{\omega \tilde{t}} &= 0 \\ \Sigma(\hat{\theta}_1 - \hat{\theta}_2) - 2\omega\hat{\theta}_1 - \omega\hat{\theta}_2 - 2\hat{\theta}_1 + \hat{\theta}_2 &= 0 \\ \Sigma(\hat{\theta}_1 - \hat{\theta}_2) - \omega(2\hat{\theta}_1 + \hat{\theta}_2) - 2\hat{\theta}_1 + \hat{\theta}_2 &= 0 \qquad (4.9) \end{aligned}$$

$$\begin{aligned} -\omega\hat{\theta}_1 e^{\omega \tilde{t}} - \omega\hat{\theta}_2 e^{\omega \tilde{t}} + \hat{\theta}_1 e^{\omega \tilde{t}} - \hat{\theta}_2 e^{\omega \tilde{t}} &= 0 \\ -\omega\hat{\theta}_1 - \omega\hat{\theta}_2 + \hat{\theta}_1 - \hat{\theta}_2 &= 0 \\ -\omega(\hat{\theta}_1 + \hat{\theta}_2) + \hat{\theta}_1 - \hat{\theta}_2 &= 0. \qquad (4.10) \end{aligned}$$

In matrix form, this is

$$\begin{bmatrix} \Sigma - 2\omega - 2 & -\Sigma - \omega + 1 \\ -\omega + 1 & -\omega - 1 \end{bmatrix} \begin{bmatrix} \hat{\theta}_1 \\ \hat{\theta}_2 \end{bmatrix} = \begin{bmatrix} 0 \\ 0 \end{bmatrix}.$$

2.2.1 Solving the Characteristic Equation

To find the non-trivial solutions, we take the determinant of the matrix and set it to zero:

$$(\Sigma - 2\omega - 2)(-1 - \omega) - (-\Sigma - \omega + 1)(1 - \omega) = 0.$$

Expanding and collecting terms yields:

$$\omega^2 + 2(3 - \Sigma)\omega + 1 = 0.$$

We solve for ω using the quadratic formula:

$$\begin{aligned} \omega_\pm &= \frac{-2(3-\Sigma) \pm \sqrt{[2(3-\Sigma)]^2 - 4(1)(1)}}{2} \\ &= \frac{-2(3-\Sigma) \pm \sqrt{4(3-\Sigma)^2 - 4}}{2} \\ &= \frac{-2(3-\Sigma) \pm \sqrt{4[(9 - 6\Sigma + \Sigma^2) - 1]}}{2} \\ &= \frac{-2(3-\Sigma) \pm \sqrt{4(\Sigma^2 - 6\Sigma + 8)}}{2} \\ &= \frac{-2(3-\Sigma) \pm 2\sqrt{(\Sigma - 4)(\Sigma - 2)}}{2}. \end{aligned}$$

We get **Equation 4.11** in [3]:

$$\omega_{\pm} = \Sigma - 3 \pm \sqrt{(\Sigma-4)(\Sigma-2)}. \tag{4.11}$$

Using Equation 4.11, we can analyze the dynamics of the Two-Link system. The paper found that if $\Sigma \leq 2$, then $\omega_{\pm} < 0$, and the system is stable. If $2 < \Sigma < 3$, $\mathrm{Re}(\omega_{\pm}) < 0$ and $\mathrm{Im}(\omega_{\pm}) \neq 0$, then the perturbations die away in an oscillatory manner. If $\Sigma = 3$, then $\mathrm{Re}(\omega_{\pm}) = 0$ and $\mathrm{Im}(\omega_{\pm}) \neq 0$, then the system is stable and shows periodic oscillations with constant amplitude. For $3 < \Sigma < 4$, $\mathrm{Re}(\omega_{\pm}) > 0$ and $\mathrm{Im}(\omega_{\pm}) \neq 0$, and thus we have that small perturbations grow exponentially with oscillations. And finally, when $\Sigma \geq 4$, $\omega_{\pm} > 0$, the system is unstable and θ_1, θ_2 so small perturbations grow exponentially without oscillation.

These results can be seen in our graphs and simulations, shown in Figure 2. Notice that when $\Sigma = 2.5$, the initial angle perturbations die out over time. When $\Sigma = 3$, the system falls into a steady oscillatory motion, and the angles oscillate with a constant amplitude. Then, when $\Sigma = 3.5$, the graph shows exponentially growing oscillations in the two-link cilium.

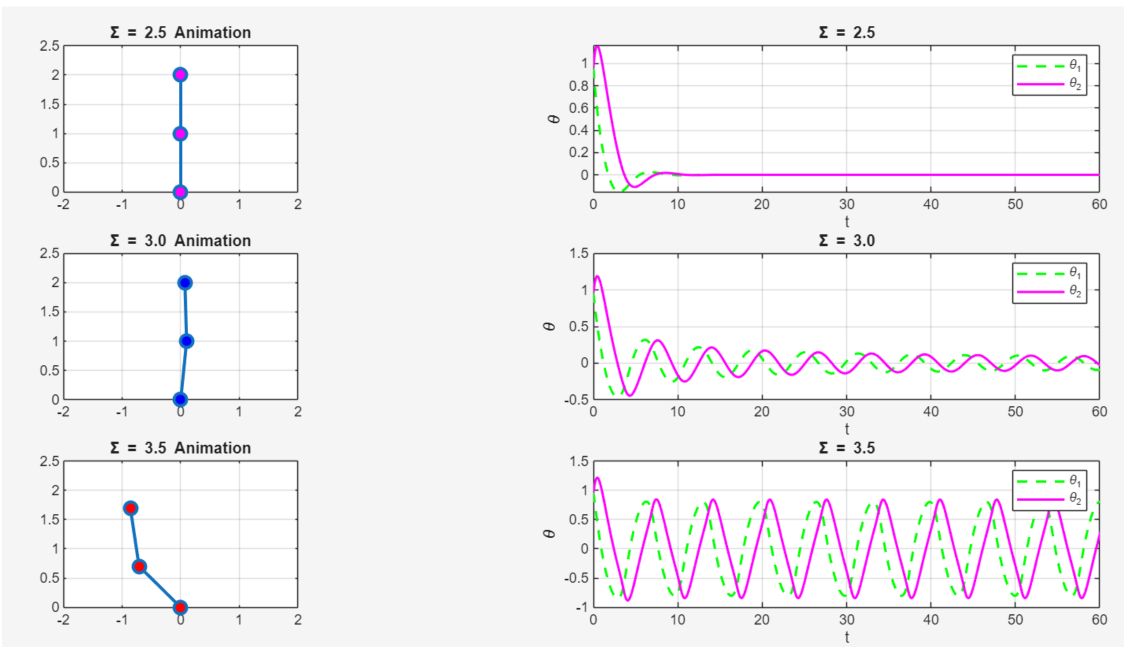

Figure 2: Two-link simulations. Left side shows the filament model and right side shows the angles θ_1 and θ_2 as functions of time

3 2-Link Coupled Follower Model

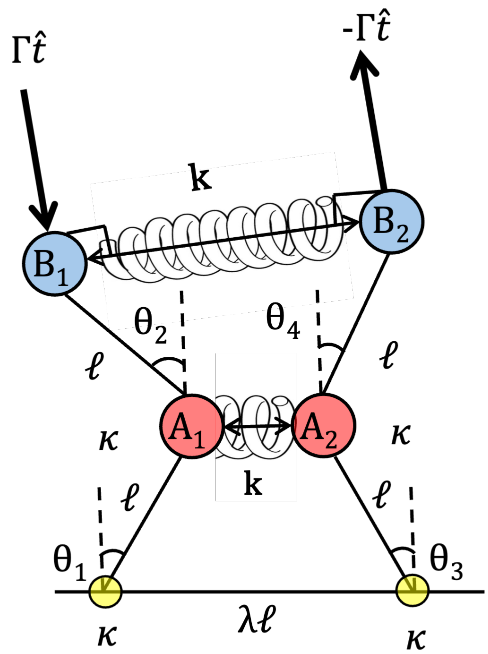

Figure 3: The set up for the coupled-2-Link Coupled Follower Model. Two filaments, both modeled as comprising of two links with length l connected by torsional springs of spring constant κ, are connected by two linear springs with spring constant k. The two filaments are acted upon by equal and opposite forces $\Gamma\hat{t}$ and $-\Gamma\hat{t}$. These forces are both perpendicular to the vector connecting the top portions of the doublets $(B_2 - B_1)$.

Cilia beating originates from the sliding of the doublet axonemal microtubules initiated by dynein arms. In the 2-Link Coupled Follower Model, the two filaments of a doublet are connected by springs with equilibrium position at λl. These springs connect the middle (A_1 and A_2) and top (B_1 and B_2) portions of the doublets. The movement of the dynein arms are modeled as equal and opposite follower forces perpendicular to the vector connecting the top portions of the doublets $(B_2 - B_1)$ at given time t.

3.1 Derivation of the 2-Link Coupled Follower Model

All forces are similar to the 2-link Model, subject to a change in coordinates. The only exceptions are the linear springs connecting A_1 and A_2, B_1 and B_2, as well as the equal and opposite follower forces.

<u>Position vectors:</u>
$r_{A_1} = l(\sin\theta_1\,,\,\cos\theta_1)$;
$r_{B_1} = l(\sin\theta_1 + \sin\theta_2\,,\,\cos\theta_1 + \cos\theta_2)$;
$r_{A_2} = l(\sin\theta_3 + \lambda\,,\,\cos\theta_3)$;
$r_{B_2} = l(\sin\theta_3 + \sin\theta_4 + \lambda\,,\,\cos\theta_3 + \cos\theta_4)$.

<u>Virtual displacements vectors:</u>
$\delta r_{A_1} = \delta\theta_1 l(\cos\theta_1\,,\,-\sin\theta_1)$;
$\delta r_{B_1} = l[\delta\theta_1(\cos\theta_1, -\sin\theta_1) + \delta\theta_2(\cos\theta_2, -\sin\theta_2)]$;
$\delta r_{A_2} = \delta\theta_3(\cos\theta_3\,,\,-\sin\theta_3)$;
$\delta r_{B_1} = l[\delta\theta_3(\cos\theta_3, -\sin\theta_3) + \delta\theta_4(\cos\theta_4, -\sin\theta_4)]$.

Velocity vectors:
$v_{A_1} = \dot{\theta}_1 l(\cos\theta_1\,,\,-\sin\theta_1)\,$;
$v_{B_1} = l[\dot{\theta}_1(\cos\theta_1\,,\,-\sin\theta_1) + \dot{\theta}_2(\cos\theta_2\,,\,-\sin\theta_2)]\,$;
$v_{A_2} = \dot{\theta}_3 l(\cos\theta_3\,,\,-\sin\theta_3)\,$;
$v_{B_2} = l[\dot{\theta}_3(\cos\theta_3\,,\,-\sin\theta_3) + \dot{\theta}_4(\cos\theta_4\,,\,-\sin\theta_4)]$.

Applied forces:
$\Gamma_{B_1} = \frac{1}{|r_{B_2}-r_{B_1}|}(r_{B_{1y}} - r_{B_{2y}}, r_{B_{2x}} - r_{B_{1x}})$;
$\Gamma_{B_2} = -\Gamma_{B_2}$.

Linear spring forces:
$F_{spr_{A_1A_2}} = -k(|r_{A_2} - r_{A_1}| - \lambda l)\frac{r_{A_2}-r_{A_1}}{|r_{A_2}-r_{A_1}|}$;
$F_{spr_{B_1B_2}} = -k(|r_{B_2} - r_{B_1}| - \lambda l)\frac{r_{B_2}-r_{B_1}}{|r_{B_2}-r_{B_1}|}$.

Torsional spring forces:
$F_{spr_{O_1}} = -\kappa\theta_1$;
$F_{spr_{O_2}} = -\kappa\theta_3$;
$F_{spr_{A_1}} = -\kappa(\theta_2 - \theta_1)$;
$F_{spr_{A_1}} = -\kappa(\theta_4 - \theta_3)$.

Drag forces:
$F_{A_1} = \zeta v_{A_1}$;
$F_{B_1} = \zeta v_{B_1}$;
$F_{A_2} = \zeta v_{A_2}$;
$F_{B_2} = \zeta v_{B_2}$.

The virtual work equation becomes:

$$\begin{aligned}\delta W = &\Gamma_{B_1}\delta r_{B_1} + \Gamma_{B_2}\delta r_{B_2}\\ &+ F_{\text{spr}_{A_1A_2}}\delta(r_{A_2} - r_{A_1}) + F_{\text{spr}_{B_1B_2}}\delta(r_{B_2} - r_{B_1})\\ &+ F_{A_1}\delta r_{A_1} + F_{A_2}\delta r_{A_2} + F_{B_1}\delta r_{B_1} + F_{B_2}\delta r_{B_2}\\ &+ F_{\text{spr}_{O_1}}\delta\theta_1 + F_{\text{spr}_{O_2}}\delta\theta_2 + F_{\text{spr}_{A_1}}\delta(\theta_2 - \theta_1) + F_{\text{spr}_{A_1}}\delta(\theta_4 - \theta_3) = 0\end{aligned}$$

After some simplification, and substituting non-dimensional parameters $\Sigma = \frac{l\Gamma}{\kappa}$ and $K = \frac{kl^2}{\kappa}$, the follow equations of motion are obtained:

$$\frac{d\theta}{dt} = f(\theta) = -A^{-1}B$$

where the symmetric matrix A is given by:

$$A = \begin{bmatrix} 2 & \cos(\theta_1 - \theta_2) & 0 & 0 \\ \cos(\theta_1 - \theta_2) & 1 & 0 & 0 \\ 0 & 0 & 2 & \cos(\theta_4 - \theta_3) \\ 0 & 0 & \cos(\theta_4 - \theta_3) & 1 \end{bmatrix}$$

and the vector $B = \begin{bmatrix} B_1 & B_2 & B_3 & B_4 \end{bmatrix}^T$ has the following components:

$$
\begin{aligned}
B_1 = \, & \frac{\Sigma}{|r_{B_2} - r_{B_1}|}\Big(-1 - \cos(\theta_2 - \theta_1) + \cos(\theta_3 - \theta_1) + \cos(\theta_4 - \theta_1) + l \sin\theta_1 \Big) + 2\theta_1 - \theta_2 \\
& - (K - \frac{K\lambda}{|r_{B_2} - r_{B_1}|})\Big(\sin(\theta_3 - \theta_1) + \sin(\theta_4 - \theta_1) + \sin(\theta_1 - \theta_2) + l \cos\theta_1 \Big) \\
& - (K - \frac{K\lambda}{|r_{A_2} - r_{A_1}|})\Big(\sin(\theta_3 - \theta_1) + l \cos\theta_1 \Big),
\end{aligned}
$$

$$
\begin{aligned}
B_2 = \, & \frac{\Sigma}{|r_{B_2} - r_{B_1}|}\Big(-1 - \cos(\theta_2 - \theta_1) + \cos(\theta_3 - \theta_2) + \cos(\theta_4 - \theta_2) + l \sin\theta_2 \Big) + \theta_2 - \theta_1 \\
& - (K - \frac{K\lambda}{|r_{B_2} - r_{B_1}|})\Big(\sin(\theta_3 - \theta_2) + \sin(\theta_4 - \theta_2) + \sin(\theta_2 - \theta_1) + l \cos\theta_2 \Big),
\end{aligned}
$$

$$
\begin{aligned}
B_3 = \, & \frac{\Sigma}{|r_{B_2} - r_{B_1}|}\Big(-1 - \cos(\theta_4 - \theta_3) + \cos(\theta_3 - \theta_2) + \cos(\theta_3 - \theta_1) - l \sin\theta_3 \Big) + 2\theta_3 - \theta_4 \\
& - (K - \frac{K\lambda}{|r_{B_2} - r_{B_1}|})\Big(\sin(\theta_3 - \theta_4) + \sin(\theta_1 - \theta_3) + \sin(\theta_2 - \theta_3) - l \cos\theta_3 \Big) \\
& - (K - \frac{K\lambda}{|r_{A_2} - r_{A_1}|})\Big(\sin(\theta_1 - \theta_3) - l \cos\theta_3 \Big),
\end{aligned}
$$

$$
\begin{aligned}
B_4 = \, & \frac{\Sigma}{|r_{B_2} - r_{B_1}|}\Big(-1 - \cos(\theta_4 - \theta_3) + \cos(\theta_4 - \theta_2) + \cos(\theta_4 - \theta_1) - l \sin\theta_4 \Big) + \theta_4 - \theta_3 \\
& - (K - \frac{K\lambda}{|r_{B_2} - r_{B_1}|})\Big(\sin(\theta_4 - \theta_3) + \sin(\theta_1 - \theta_4) + \sin(\theta_2 - \theta_4) - l \cos\theta_4 \Big).
\end{aligned}
$$

3.2 Bifurcation analysis

The Jacobian of $f(\theta)$ at the equilibrium position (the origin) is given by:

$$
J = \begin{bmatrix}
-k - \Sigma - 3 & \Sigma + 2 & K & 0 \\
\Sigma + 4 & -K - 2\Sigma - 3 & 0 & K \\
K & 0 & \Sigma - K - 3 & 2 - \Sigma \\
0 & K & 4 - \Sigma & 2\Sigma - K - 3
\end{bmatrix}
$$

The eigenvalues of the Jacobian are found to be real regardless of parameter values. However, there exist saddle-node bifurcations that exhibit global oscillatory behavior.

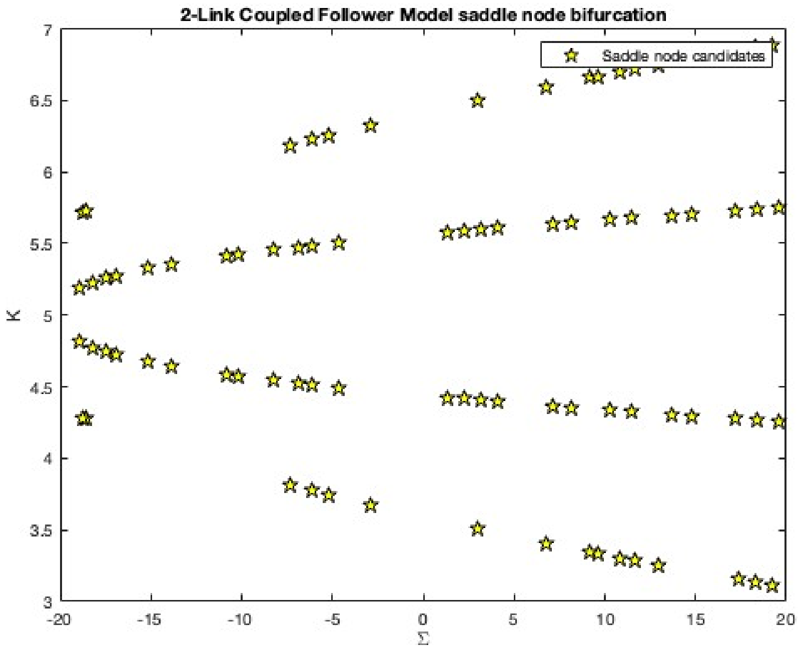

Figure 4: Potential candidates of (Σ, K) that yield a saddle node bifurcation for the 2-Link Coupled Follower Model.

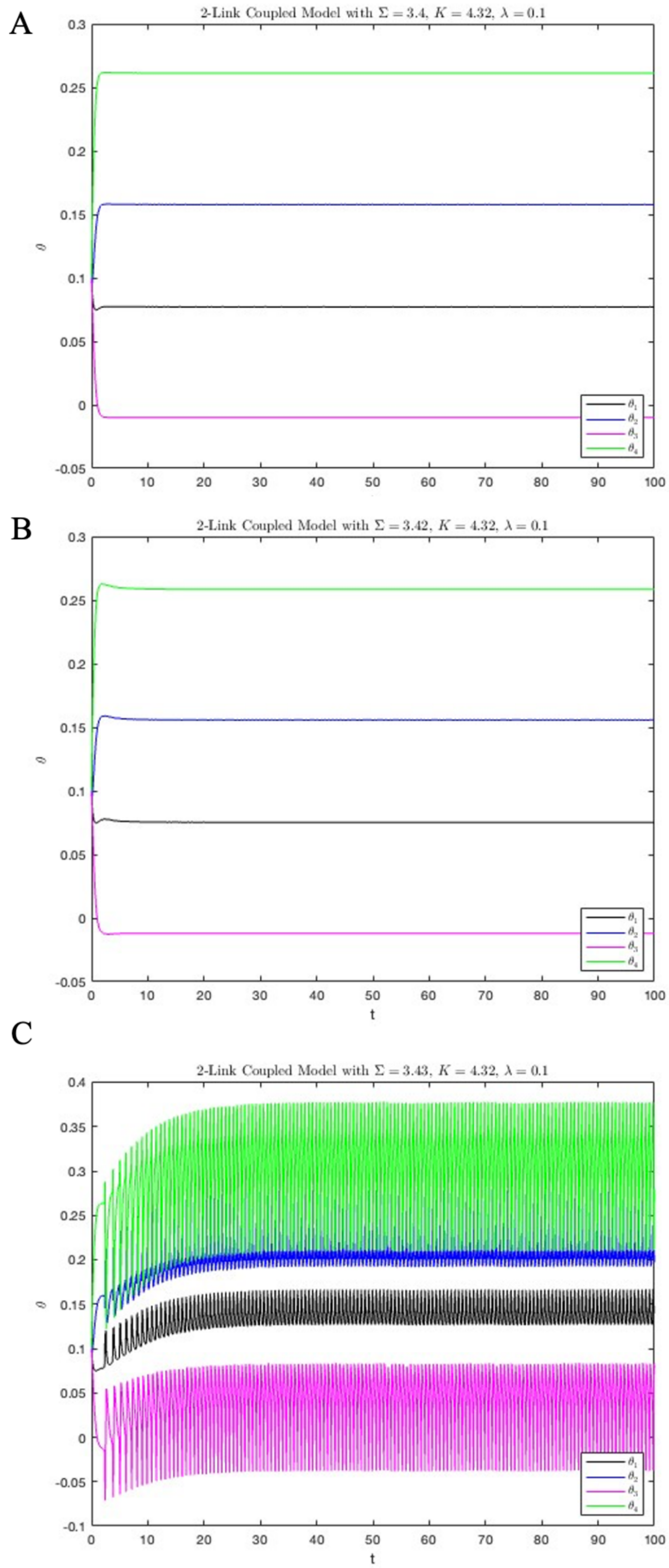

Figure 5: Trajectories of the 2-Link Coupled Follower Model around the bifurcation point given by $\Sigma = 3.42$ and $K = 4.32$

4 2-Link Extension to Three Dimensions

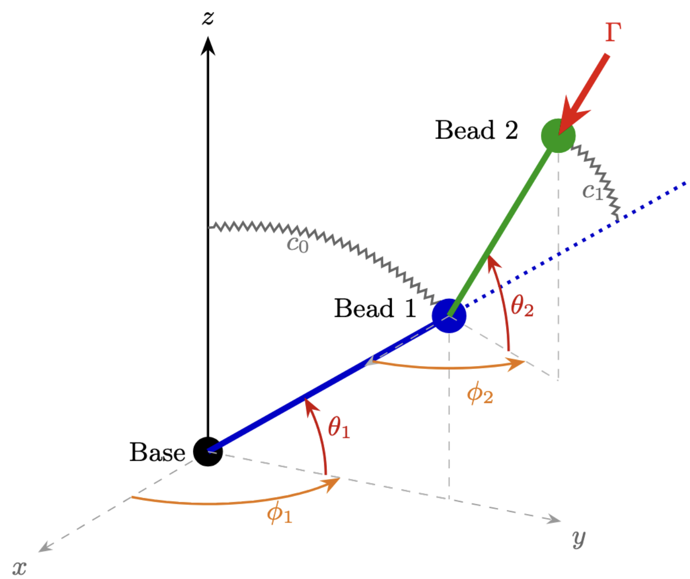

Figure 6: Two Link Model in 3D

[]

- ϕ_1, ϕ_2 **(Azimuthal Angles / Planar Sweeps):** These parameters represent the horizontal orientation of each link in the xy-plane.
- θ_1, θ_2 **(Elevation Angles):** These measure the vertical tilt of the links. Each angle tracks a vertical sweeping arc that lifts upward directly from the horizontal xy-plane (or some other local reference plane parallel to the xy plane) up to the respective link segment.
- c_0 **(Base Bending Angle):** Measures how much Link 1 tilts away from the vertical z-axis (e_3)
- c_1 **(Intermediate Joint Bending Angle):** Measures the relative bending between the two successive link segments
- Γ **(The Compressive Follower Force)**

We model the elastic filament as a **two-link chain**: clamped at origin $\boldsymbol{r}_0 = \mathbf{0}$, beads at $\boldsymbol{r}_1$ and $\boldsymbol{r}_2$, connected by rigid inextensible links of equal length $\ell = L/2$.

The unit tangent to link i is

$$\boldsymbol{t}_i = \frac{\boldsymbol{r}_i - \boldsymbol{r}_{i-1}}{|\boldsymbol{r}_i - \boldsymbol{r}_{i-1}|}, \qquad i = 1, 2, \tag{1}$$

and inextensibility requires $|\boldsymbol{r}_i - \boldsymbol{r}_{i-1}| = \ell$ at all times.

Each link direction is parameterised by **spherical coordinates** (θ_i, ϕ_i):

$$\boldsymbol{t}_i(\theta_i, \phi_i) = \begin{pmatrix} \cos\theta_i \cos\phi_i \\ \cos\theta_i \sin\phi_i \\ \sin\theta_i \end{pmatrix}, \qquad \theta_i \in \left(-\tfrac{\pi}{2}, \tfrac{\pi}{2}\right), \quad \phi_i \in [0, 2\pi). \tag{2}$$

The bead positions follow immediately:

$$\boldsymbol{r}_1 = \ell\, \boldsymbol{t}_1, \qquad \boldsymbol{r}_2 = \ell\, \boldsymbol{t}_1 + \ell\, \boldsymbol{t}_2. \tag{3}$$

The generalised coordinates are $\boldsymbol{q} = (\theta_1, \phi_1, \theta_2, \phi_2)^\mathsf{T} \in \mathbb{R}^4$.

4.1 Kinematics and virtual displacements

To calculate the velocities of each bead in terms of our generalised coordinates we will use chain rule, and thus will need partial derivatives of the links' tangent vectors with respect to the corresponding angles of that link:

$$\hat{\boldsymbol{e}}_{\theta_i} := \frac{\partial \boldsymbol{t}_i}{\partial \theta_i} = \begin{pmatrix} -\sin\theta_i \cos\phi_i \\ -\sin\theta_i \sin\phi_i \\ \cos\theta_i \end{pmatrix}, \qquad \hat{\boldsymbol{e}}_{\phi_i} := \frac{\partial \boldsymbol{t}_i}{\partial \phi_i} = \begin{pmatrix} -\cos\theta_i \sin\phi_i \\ \cos\theta_i \cos\phi_i \\ 0 \end{pmatrix}. \tag{4}$$

Note the orthogonality relations $\hat{\boldsymbol{e}}_{\theta_i} \perp \boldsymbol{t}_i$, $\hat{\boldsymbol{e}}_{\phi_i} \perp \boldsymbol{t}_i$, and $\hat{\boldsymbol{e}}_{\theta_i} \cdot \hat{\boldsymbol{e}}_{\phi_i} = 0$.
The velocities of the beads are

$$\dot{\boldsymbol{r}}_1 = \ell\big(\hat{\boldsymbol{e}}_{\theta_1}\dot{\theta}_1 + \hat{\boldsymbol{e}}_{\phi_1}\dot{\phi}_1\big), \qquad \dot{\boldsymbol{r}}_2 = \dot{\boldsymbol{r}}_1 + \ell\big(\hat{\boldsymbol{e}}_{\theta_2}\dot{\theta}_2 + \hat{\boldsymbol{e}}_{\phi_2}\dot{\phi}_2\big). \tag{5}$$

The virtual displacements of each bead have the same form with $\delta\theta_i, \delta\phi_i$ replacing $\dot{\theta}_i, \dot{\phi}_i$:

$$\delta\boldsymbol{r}_1 = \ell\big(\hat{\boldsymbol{e}}_{\theta_1}\,\delta\theta_1 + \hat{\boldsymbol{e}}_{\phi_1}\,\delta\phi_1\big), \tag{6}$$

$$\delta\boldsymbol{r}_2 = \ell\big(\hat{\boldsymbol{e}}_{\theta_1}\,\delta\theta_1 + \hat{\boldsymbol{e}}_{\phi_1}\,\delta\phi_1\big) + \ell\big(\hat{\boldsymbol{e}}_{\theta_2}\,\delta\theta_2 + \hat{\boldsymbol{e}}_{\phi_2}\,\delta\phi_2\big). \tag{7}$$

4.2 Forces and moments

4.2.1 Drag Force

Drag force on each bead j :

$$\boldsymbol{F}_{h,j} = -\zeta\,\dot{\boldsymbol{r}}_j, \qquad j = 1, 2 \tag{8}$$

where $\zeta > 0$ is the drag coefficient.

4.2.2 Applied follower force

A compressive follower force acts on bead 2 along the current direction of link 2:

$$\boldsymbol{\Gamma} = -F_a\,\boldsymbol{t}_2. \tag{9}$$

where F_a is the magnitude of the follower force.

4.2.3 Elastic spring moments

Two torsional springs of stiffness K resist bending:

Location	Bending angle
Base/Bead 0	$c_0 = \cos^{-1}(\boldsymbol{e}_3 \cdot \boldsymbol{t}_1) = \pi/2 - \theta_1$
Bead 1 (joint)	$c_1 = \cos^{-1}(\boldsymbol{t}_1 \cdot \boldsymbol{t}_2)$

The restoring force at joint i has magnitude Kc_i, and the spring's virtual work is $-Kc_i\,\delta c_i$.

4.2.4 Differentials of the bending angles

Base spring. Since $c_0 = \pi/2 - \theta_1$, we have immediately

$$\delta c_0 = -\delta\theta_1. \tag{10}$$

Joint spring. Differentiating $\cos c_1 = \boldsymbol{t}_1 \cdot \boldsymbol{t}_2$ gives $-\sin c_1\,\delta c_1 = \delta\boldsymbol{t}_1 \cdot \boldsymbol{t}_2 + \boldsymbol{t}_1 \cdot \delta\boldsymbol{t}_2$. Expanding:

$$-\sin c_1\,\delta c_1 = \big(\hat{\boldsymbol{e}}_{\theta_1} \cdot \boldsymbol{t}_2\big)\delta\theta_1 + \big(\hat{\boldsymbol{e}}_{\phi_1} \cdot \boldsymbol{t}_2\big)\delta\phi_1 + \big(\boldsymbol{t}_1 \cdot \hat{\boldsymbol{e}}_{\theta_2}\big)\delta\theta_2 + \big(\boldsymbol{t}_1 \cdot \hat{\boldsymbol{e}}_{\phi_2}\big)\delta\phi_2. \tag{11}$$

4.3 Principle of virtual work

In the low Reynolds (overdamped/Stokes) regime, inertia is neglected. Using the principle of virtual work for differentials $(\delta\theta_1, \delta\phi_1, \delta\theta_2, \delta\phi_2)$:

$$\boldsymbol{F}_a \cdot \delta \boldsymbol{r}_2 + \sum_{j=1}^{2} \boldsymbol{F}_{h,j} \cdot \delta \boldsymbol{r}_j - Kc_0\,\delta c_0 - Kc_1\,\delta c_1 = 0. \tag{12}$$

4.3.1 Drag virtual work

Rewrite bead velocities. The velocities $\dot{\boldsymbol{r}}_j$ are linear in $\dot{\boldsymbol{q}}$; the same linear map sends $\delta\boldsymbol{q} \mapsto \delta\boldsymbol{r}_j$. Writing this map as a 3×4 matrix J_j (columns indexed by $\theta_1, \phi_1, \theta_2, \phi_2$):

$$\dot{\boldsymbol{r}}_j = J_j\,\dot{\boldsymbol{q}}, \qquad \delta\boldsymbol{r}_j = J_j\,\delta\boldsymbol{q}, \tag{13}$$

where, from the velocity expressions in §4.1:

$$J_1 = \ell\begin{pmatrix}\hat{\boldsymbol{e}}_{\theta_1} & \hat{\boldsymbol{e}}_{\phi_1} & \boldsymbol{0} & \boldsymbol{0}\end{pmatrix}, \qquad J_2 = \ell\begin{pmatrix}\hat{\boldsymbol{e}}_{\theta_1} & \hat{\boldsymbol{e}}_{\phi_1} & \hat{\boldsymbol{e}}_{\theta_2} & \hat{\boldsymbol{e}}_{\phi_2}\end{pmatrix}. \tag{14}$$

(Each displayed entry is a 3-vector, so $J_j \in \mathbb{R}^{3\times4}$.) Bead 1 moves only with link-1 angles; bead 2 moves with both links.

Each bead's contribution is an outer-product matrix. The drag virtual work of bead j is

$$-\zeta\,\dot{\boldsymbol{r}}_j \cdot \delta\boldsymbol{r}_j = -\zeta\,(J_j\dot{\boldsymbol{q}})\cdot(J_j\delta\boldsymbol{q}) = -\zeta\,\dot{\boldsymbol{q}}^{\mathsf{T}}(J_j^{\mathsf{T}}J_j)\,\delta\boldsymbol{q}. \tag{15}$$

Summing over both beads:

$$\sum_{j=1}^{2}\boldsymbol{F}_{h,j}\cdot\delta\boldsymbol{r}_j = -\dot{\boldsymbol{q}}^{\mathsf{T}}\left(\zeta\sum_{j=1}^{2}J_j^{\mathsf{T}}J_j\right)\delta\boldsymbol{q} =: -\dot{\boldsymbol{q}}^{\mathsf{T}}\boldsymbol{D}\,\delta\boldsymbol{q}, \tag{16}$$

so the drag matrix is

$$\boldsymbol{D} = \zeta\big(J_1^{\mathsf{T}}J_1 + J_2^{\mathsf{T}}J_2\big). \tag{17}$$

D is Symmetric and Positive Definite: Symmetry ($\boldsymbol{D} = \boldsymbol{D}^{\mathsf{T}}$) follows immediately since each $J_j^{\mathsf{T}}J_j$ is symmetric. For positive definiteness, take any $\boldsymbol{v} \in \mathbb{R}^4$, $\boldsymbol{v} \neq \boldsymbol{0}$:

$$\boldsymbol{v}^{\mathsf{T}}\boldsymbol{D}\,\boldsymbol{v} = \zeta\sum_{j=1}^{2}\boldsymbol{v}^{\mathsf{T}}J_j^{\mathsf{T}}J_j\,\boldsymbol{v} = \zeta\sum_{j=1}^{2}\|J_j\boldsymbol{v}\|^2 \;\geq\; 0, \tag{18}$$

so $\boldsymbol{D}$ is at least positive semi-definite. It is strictly positive definite if and only if $J_j\boldsymbol{v} = \boldsymbol{0}$ for both $j = 1, 2$ implies $\boldsymbol{v} = \boldsymbol{0}$, i.e. the combined column space condition

$$\ker J_1 \cap \ker J_2 = \{\boldsymbol{0}\}. \tag{19}$$

From eq. (14), the columns of J_1 are $\ell\,\hat{\boldsymbol{e}}_{\theta_1}$ and $\ell\,\hat{\boldsymbol{e}}_{\phi_1}$ (in positions 1,2) with zeros elsewhere, so

$$J_1\boldsymbol{v} = \ell\,(v_1\,\hat{\boldsymbol{e}}_{\theta_1} + v_2\,\hat{\boldsymbol{e}}_{\phi_1}), \tag{20}$$

which vanishes only when $v_1 = v_2 = 0$, since $\{\hat{\boldsymbol{e}}_{\theta_1}, \hat{\boldsymbol{e}}_{\phi_1}\}$ are linearly independent (they are orthogonal unit vectors on the sphere). Thus $\ker J_1 = \{\boldsymbol{v} : v_1 = v_2 = 0\}$.

So now considering the portion kernel space of J_2 where J_1 also has zeroes:

$$J_2\boldsymbol{v} = \ell\,(v_1\,\hat{\boldsymbol{e}}_{\theta_1} + v_2\,\hat{\boldsymbol{e}}_{\phi_1} + v_3\,\hat{\boldsymbol{e}}_{\theta_2} + v_4\,\hat{\boldsymbol{e}}_{\phi_2}) = \ell\,(v_3\,\hat{\boldsymbol{e}}_{\theta_2} + v_4\,\hat{\boldsymbol{e}}_{\phi_2}), \tag{21}$$

which vanishes only when the other two coefficients are zero as well (i.e. $\{v_3 = v_4 = 0\}$), since $\{\hat{\boldsymbol{e}}_{\theta_2}, \hat{\boldsymbol{e}}_{\phi_2}\}$ are linearly independent (because orthogonal by eq. (7)). Thus $\ker J_1 \cap \ker J_2 = \{\boldsymbol{0}\}$, and condition (19) is satisfied. Therefore $\boldsymbol{D}$ is *positive definite*, thus D is invertible.

Viewing D as blocks of relations between beads: D is a 4 by 4 matrix and we consider as a 2 by 2 block of 2 by 2 submatrices. Each of these submatrices represent some relation amongst the beads. The (1,1) block is relation of bead 1 angles $\{\theta_1,\ \phi_1\}$ with themselves. The (2,2) block is relation of bead 2 angles amongst themselves. The (1,2) and (2,1) blocks are the same (just transposed) and represent relation between angles across the 2 different beads.

Computing $J_1^\top J_1$. The (k,l) entry of $J_j^\top J_j$ is the dot product of columns k and l of J_j. Since J_1 has non-zero columns only in positions (θ_1, ϕ_1), the matrix $J_1^\top J_1$ is non-zero only in the $(1,1)$ block. Using $|\hat{\boldsymbol{e}}_{\theta_1}|^2 = 1$, $|\hat{\boldsymbol{e}}_{\phi_1}|^2 = \cos^2\theta_1$, and $\hat{\boldsymbol{e}}_{\theta_1} \cdot \hat{\boldsymbol{e}}_{\phi_1} = 0$:

$$J_1^\top J_1 = \ell^2 \begin{pmatrix} 1 & 0 & 0 & 0 \\ 0 & \cos^2\theta_1 & 0 & 0 \\ 0 & 0 & 0 & 0 \\ 0 & 0 & 0 & 0 \end{pmatrix}. \tag{22}$$

Computing $J_2^\top J_2$. All four columns of J_2 are non-zero, so all 4×4 entries contribute. Using $|\hat{\boldsymbol{e}}_{\theta_i}|^2 = 1$, $|\hat{\boldsymbol{e}}_{\phi_i}|^2 = \cos^2\theta_i$, $\hat{\boldsymbol{e}}_{\theta_i} \cdot \hat{\boldsymbol{e}}_{\phi_i} = 0$ for each i, and the inter-link dot products as they appear:

$$J_2^\top J_2 = \ell^2 \begin{pmatrix} 1 & 0 & \hat{\boldsymbol{e}}_{\theta_1} \cdot \hat{\boldsymbol{e}}_{\theta_2} & \hat{\boldsymbol{e}}_{\theta_1} \cdot \hat{\boldsymbol{e}}_{\phi_2} \\ 0 & \cos^2\theta_1 & \hat{\boldsymbol{e}}_{\phi_1} \cdot \hat{\boldsymbol{e}}_{\theta_2} & \hat{\boldsymbol{e}}_{\phi_1} \cdot \hat{\boldsymbol{e}}_{\phi_2} \\ \hat{\boldsymbol{e}}_{\theta_2} \cdot \hat{\boldsymbol{e}}_{\theta_1} & \hat{\boldsymbol{e}}_{\theta_2} \cdot \hat{\boldsymbol{e}}_{\phi_1} & 1 & 0 \\ \hat{\boldsymbol{e}}_{\phi_2} \cdot \hat{\boldsymbol{e}}_{\theta_1} & \hat{\boldsymbol{e}}_{\phi_2} \cdot \hat{\boldsymbol{e}}_{\phi_1} & 0 & \cos^2\theta_2 \end{pmatrix}. \tag{23}$$

Summing the two matrices. Adding eq. (22) and eq. (23) according to eq. (17):

$$\boldsymbol{D} = \zeta\ell^2 \begin{pmatrix} 2 & 0 & \hat{\boldsymbol{e}}_{\theta_1} \cdot \hat{\boldsymbol{e}}_{\theta_2} & \hat{\boldsymbol{e}}_{\theta_1} \cdot \hat{\boldsymbol{e}}_{\phi_2} \\ 0 & 2\cos^2\theta_1 & \hat{\boldsymbol{e}}_{\phi_1} \cdot \hat{\boldsymbol{e}}_{\theta_2} & \hat{\boldsymbol{e}}_{\phi_1} \cdot \hat{\boldsymbol{e}}_{\phi_2} \\ \hat{\boldsymbol{e}}_{\theta_2} \cdot \hat{\boldsymbol{e}}_{\theta_1} & \hat{\boldsymbol{e}}_{\theta_2} \cdot \hat{\boldsymbol{e}}_{\phi_1} & 1 & 0 \\ \hat{\boldsymbol{e}}_{\phi_2} \cdot \hat{\boldsymbol{e}}_{\theta_1} & \hat{\boldsymbol{e}}_{\phi_2} \cdot \hat{\boldsymbol{e}}_{\phi_1} & 0 & \cos^2\theta_2 \end{pmatrix}. \tag{24}$$

The factor of 2 in the $(1,1)$ block arises because bead 1 contributes via $J_1^\top J_1$ and bead 2 also contributes the same block via $J_2^\top J_2$ (both beads lie downstream of link 1). The $(2,2)$ block carries no factor of 2 since only bead 2 lies downstream of link 2. The off-diagonal $(1,2)$ and $(2,1)$ blocks come entirely from $J_2^\top J_2$.

4.4 Follower force virtual work

Using eq. (7):

$$\boldsymbol{F}_a \cdot \delta\boldsymbol{r}_2 = -F_a \boldsymbol{t}_2 \cdot \Big[\ell\big(\hat{\boldsymbol{e}}_{\theta_1}\delta\theta_1 + \hat{\boldsymbol{e}}_{\phi_1}\delta\phi_1\big) + \ell\big(\hat{\boldsymbol{e}}_{\theta_2}\delta\theta_2 + \hat{\boldsymbol{e}}_{\phi_2}\delta\phi_2\big)\Big]. \tag{25}$$

Because $\boldsymbol{t}_2 \perp \hat{\boldsymbol{e}}_{\theta_2}$ and $\boldsymbol{t}_2 \perp \hat{\boldsymbol{e}}_{\phi_2}$, the second bracket vanishes:

$$\boldsymbol{F}_a \cdot \delta\boldsymbol{r}_2 = -F_a\ell\Big[\big(\boldsymbol{t}_2 \cdot \hat{\boldsymbol{e}}_{\theta_1}\big)\delta\theta_1 + \big(\boldsymbol{t}_2 \cdot \hat{\boldsymbol{e}}_{\phi_1}\big)\delta\phi_1\Big]. \tag{26}$$

4.5 Spring virtual work

The total spring virtual work is $-Kc_0\,\delta c_0 - Kc_1\,\delta c_1$. Using $\delta c_0 = -\delta\theta_1$ and eq. (11):

$$-Kc_0\,\delta c_0 = Kc_0\,\delta\theta_1, \tag{27}$$

$$-Kc_1\,\delta c_1 = \frac{Kc_1}{\sin c_1}\Big[\big(\hat{\boldsymbol{e}}_{\theta_1} \cdot \boldsymbol{t}_2\big)\delta\theta_1 + \big(\hat{\boldsymbol{e}}_{\phi_1} \cdot \boldsymbol{t}_2\big)\delta\phi_1 + \big(\boldsymbol{t}_1 \cdot \hat{\boldsymbol{e}}_{\theta_2}\big)\delta\theta_2 + \big(\boldsymbol{t}_1 \cdot \hat{\boldsymbol{e}}_{\phi_2}\big)\delta\phi_2\Big]. \tag{28}$$

4.6 Full nonlinear equations of motion

We now collect all three virtual work contributions from eq. (12) and write each as $(\cdots)\delta\boldsymbol{q}$

Drag term (from §4.3.1). Already in the required form:

$$\sum_{j=1}^{2} \boldsymbol{F}_{h,j} \cdot \delta \boldsymbol{r}_j = -\dot{\boldsymbol{q}}^{\mathsf{T}} \boldsymbol{D}\, \delta \boldsymbol{q}. \tag{29}$$

Follower-force term. From eq. (26), the follower force contributes only to the link-1 angle slots. Introducing the 4-vector

$$\boldsymbol{p}(\boldsymbol{q}) \coloneqq -F_a \ell \begin{pmatrix} \boldsymbol{t}_2 \cdot \hat{\boldsymbol{e}}_{\theta_1} \\ \boldsymbol{t}_2 \cdot \hat{\boldsymbol{e}}_{\phi_1} \\ 0 \\ 0 \end{pmatrix} = -F_a \ell\, J_2^{\mathsf{T}} \boldsymbol{t}_2, \tag{30}$$

we can rewrite follower force work as

$$\boldsymbol{F}_a \cdot \delta \boldsymbol{r}_2 = \boldsymbol{p}(\boldsymbol{q})^{\mathsf{T}} \delta \boldsymbol{q}. \tag{31}$$

To see why the last two entries of $\boldsymbol{p}$ vanish, note that $J_2^{\mathsf{T}} \boldsymbol{t}_2$ would give $\ell(\hat{\boldsymbol{e}}_{\theta_1} \cdot \boldsymbol{t}_2,\ \hat{\boldsymbol{e}}_{\phi_1} \cdot \boldsymbol{t}_2,\ \hat{\boldsymbol{e}}_{\theta_2} \cdot \boldsymbol{t}_2,\ \hat{\boldsymbol{e}}_{\phi_2} \cdot \boldsymbol{t}_2)^{\mathsf{T}}$, but $\hat{\boldsymbol{e}}_{\theta_2} \cdot \boldsymbol{t}_2 = \hat{\boldsymbol{e}}_{\phi_2} \cdot \boldsymbol{t}_2 = 0$, so the last two entries are exactly zero.

Spring term. Define the gradient of each bending angle with respect to $\boldsymbol{q}$:

$$\nabla_{\boldsymbol{q}} c_0 = \begin{pmatrix} -1 \\ 0 \\ 0 \\ 0 \end{pmatrix}, \qquad \nabla_{\boldsymbol{q}} c_1 = -\frac{1}{\sin c_1} \begin{pmatrix} \hat{\boldsymbol{e}}_{\theta_1} \cdot \boldsymbol{t}_2 \\ \hat{\boldsymbol{e}}_{\phi_1} \cdot \boldsymbol{t}_2 \\ \boldsymbol{t}_1 \cdot \hat{\boldsymbol{e}}_{\theta_2} \\ \boldsymbol{t}_1 \cdot \hat{\boldsymbol{e}}_{\phi_2} \end{pmatrix}, \tag{32}$$

where $\nabla_{\boldsymbol{q}} c_0$ follows from $\delta c_0 = -\delta\theta_1$, and $\nabla_{\boldsymbol{q}} c_1$ similarly follows from eq. (11)
The total spring virtual work is then

$$-Kc_0\, \delta c_0 - Kc_1\, \delta c_1 = -Kc_0\, (\nabla_{\boldsymbol{q}} c_0)^{\mathsf{T}} \delta \boldsymbol{q} \ - \ Kc_1\, (\nabla_{\boldsymbol{q}} c_1)^{\mathsf{T}} \delta \boldsymbol{q} = \boldsymbol{s}(\boldsymbol{q})^{\mathsf{T}} \delta \boldsymbol{q}, \tag{33}$$

where s(q) is defined as:

$$\boldsymbol{s}(\boldsymbol{q}) = \begin{pmatrix} Kc_0 \\ 0 \\ 0 \\ 0 \end{pmatrix} + \frac{Kc_1}{\sin c_1} \begin{pmatrix} \hat{\boldsymbol{e}}_{\theta_1} \cdot \boldsymbol{t}_2 \\ \hat{\boldsymbol{e}}_{\phi_1} \cdot \boldsymbol{t}_2 \\ \boldsymbol{t}_1 \cdot \hat{\boldsymbol{e}}_{\theta_2} \\ \boldsymbol{t}_1 \cdot \hat{\boldsymbol{e}}_{\phi_2} \end{pmatrix}. \tag{34}$$

Assembling the virtual work balance. Substituting eqs. (29), (31) and (33) into the principle of virtual work eq. (12):

$$\left[\boldsymbol{p}(\boldsymbol{q}) + \boldsymbol{s}(\boldsymbol{q}) - \boldsymbol{D}(\boldsymbol{q})\, \dot{\boldsymbol{q}}\right]^{\mathsf{T}} \delta \boldsymbol{q} = 0 \quad \forall\, \delta \boldsymbol{q}. \tag{35}$$

For each of these four differentials of angles, we can create 4 equations of motion by just leaving one to be arbitrary and setting rest to 0:

$$\left[\boldsymbol{p}(\boldsymbol{q}) + \boldsymbol{s}(\boldsymbol{q}) - \boldsymbol{D}(\boldsymbol{q})\, \dot{\boldsymbol{q}}\right] = 0, \tag{36}$$

where 0 is the zero vector in $\mathbb{R}^4$.

Result 1 (Nonlinear equations of motion, $N = 2$)**.**

$$\boldsymbol{D}(\boldsymbol{q})\,\dot{\boldsymbol{q}} = \boldsymbol{f}(\boldsymbol{q}), \tag{37}$$

where $\boldsymbol{D}$ is given in eq. (24) and the total generalized force vector is

$$\boldsymbol{f}(\boldsymbol{q}) \coloneqq \boldsymbol{p}(\boldsymbol{q}) + \boldsymbol{s}(\boldsymbol{q}) = -F_a J_2^{\mathsf{T}} \boldsymbol{t}_2 \;+\; K c_0 \,\nabla_{\boldsymbol{q}} c_0 \;+\; K c_1 \,\nabla_{\boldsymbol{q}} c_1, \tag{38}$$

or in component form, using eqs. (30) and (34):

$$f_{\theta_1} = -F_a \ell \,(\boldsymbol{t}_2 \cdot \hat{\boldsymbol{e}}_{\theta_1}) + K c_0 + \frac{K c_1}{\sin c_1}\,(\hat{\boldsymbol{e}}_{\theta_1} \cdot \boldsymbol{t}_2), \tag{39}$$

$$f_{\phi_1} = -F_a \ell \,(\boldsymbol{t}_2 \cdot \hat{\boldsymbol{e}}_{\phi_1}) + \frac{K c_1}{\sin c_1}\,(\hat{\boldsymbol{e}}_{\phi_1} \cdot \boldsymbol{t}_2), \tag{40}$$

$$f_{\theta_2} = \frac{K c_1}{\sin c_1}\,(\boldsymbol{t}_1 \cdot \hat{\boldsymbol{e}}_{\theta_2}), \tag{41}$$

$$f_{\phi_2} = \frac{K c_1}{\sin c_1}\,(\boldsymbol{t}_1 \cdot \hat{\boldsymbol{e}}_{\phi_2}). \tag{42}$$

where $\boldsymbol{f} = (f_{\theta_1}, f_{\phi_1}, f_{\theta_2}, f_{\phi_2})^T$.

To turn these implicit ODEs into explicit form we can just invert D (remember D is PD, thus invertible).

4.7 Non-dimensionalisation of the equations of motion

Introduce time scale:

$$T_c = \frac{\zeta \ell^2}{K} \quad [\mathrm{s}], \tag{43}$$

We define dimensionless time via

$$\tau = \frac{t}{T_c} = \frac{K t}{\zeta \ell^2}. \tag{44}$$

Substituting $\mathrm{d}/\mathrm{d}t = (1/T_c)\,\mathrm{d}/\mathrm{d}\tau$ into eq. (37) and multiplying through by T_c:

$$\boldsymbol{D}(\boldsymbol{q})\,\frac{\mathrm{d}\boldsymbol{q}}{\mathrm{d}\tau} = T_c\,\boldsymbol{f}(\boldsymbol{q}). \tag{45}$$

Recalling $\boldsymbol{D} = \zeta \ell^2 \hat{\boldsymbol{D}}$ from eq. (24), the left-hand side becomes:

$$\zeta \ell^2\,\hat{\boldsymbol{D}}(\boldsymbol{q})\,\frac{\mathrm{d}\boldsymbol{q}}{\mathrm{d}\tau}, \qquad \hat{\boldsymbol{D}}(\boldsymbol{q}) = \begin{pmatrix} 2 & 0 & \hat{\boldsymbol{e}}_{\theta_1} \cdot \hat{\boldsymbol{e}}_{\theta_2} & \hat{\boldsymbol{e}}_{\theta_1} \cdot \hat{\boldsymbol{e}}_{\phi_2} \\ 0 & 2\cos^2\theta_1 & \hat{\boldsymbol{e}}_{\phi_1} \cdot \hat{\boldsymbol{e}}_{\theta_2} & \hat{\boldsymbol{e}}_{\phi_1} \cdot \hat{\boldsymbol{e}}_{\phi_2} \\ \hat{\boldsymbol{e}}_{\theta_2} \cdot \hat{\boldsymbol{e}}_{\theta_1} & \hat{\boldsymbol{e}}_{\theta_2} \cdot \hat{\boldsymbol{e}}_{\phi_1} & 1 & 0 \\ \hat{\boldsymbol{e}}_{\phi_2} \cdot \hat{\boldsymbol{e}}_{\theta_1} & \hat{\boldsymbol{e}}_{\phi_2} \cdot \hat{\boldsymbol{e}}_{\phi_1} & 0 & \cos^2\theta_2 \end{pmatrix}. \tag{46}$$

Dividing both sides of eq. (45) by $\zeta \ell^2$:

$$\hat{\boldsymbol{D}}(\boldsymbol{q})\,\frac{\mathrm{d}\boldsymbol{q}}{\mathrm{d}\tau} = \frac{T_c}{\zeta \ell^2}\,\boldsymbol{f}(\boldsymbol{q}) = \frac{1}{K}\,\boldsymbol{f}(\boldsymbol{q}). \tag{47}$$

Time to non-dimensionalise $\boldsymbol{f}$. From eqs. (39) to (42), dividing by K and introducing

$$\Sigma = \frac{F_a \ell}{K} \tag{48}$$

(ratio of follower-force torque to spring stiffness), the right-hand side $\hat{\boldsymbol{f}} \coloneqq \boldsymbol{f}/K$ becomes:

$$\hat{f}_{\theta_1} = -\Sigma\,(\boldsymbol{t}_2 \cdot \hat{\boldsymbol{e}}_{\theta_1}) + c_0 + \frac{c_1}{\sin c_1}\,(\hat{\boldsymbol{e}}_{\theta_1} \cdot \boldsymbol{t}_2), \tag{49}$$

$$\hat{f}_{\phi_1} = -\Sigma\,(\boldsymbol{t}_2 \cdot \hat{\boldsymbol{e}}_{\phi_1}) + \frac{c_1}{\sin c_1}\,(\hat{\boldsymbol{e}}_{\phi_1} \cdot \boldsymbol{t}_2), \tag{50}$$

$$\hat{f}_{\theta_2} = \frac{c_1}{\sin c_1}\,(\boldsymbol{t}_1 \cdot \hat{\boldsymbol{e}}_{\theta_2}), \tag{51}$$

$$\hat{f}_{\phi_2} = \frac{c_1}{\sin c_1}\,(\boldsymbol{t}_1 \cdot \hat{\boldsymbol{e}}_{\phi_2}). \tag{52}$$

Result 2 (Dimensionless equations of motion)**.**

$$\hat{\boldsymbol{D}}(\boldsymbol{q})\,\frac{\mathrm{d}\boldsymbol{q}}{\mathrm{d}\tau} = \hat{\boldsymbol{f}}(\boldsymbol{q};\Sigma), \tag{53}$$

After simulating this model in Matlab for many values of Σ, we observed a bifurcation around $\Sigma = 3$. Below this threshold (like at $\Sigma = 2.9$), the cilia ends up in a upright, stable position. Past this threshold (like at $\Sigma = 3.1$), the cilia ends up in a stable cycle.

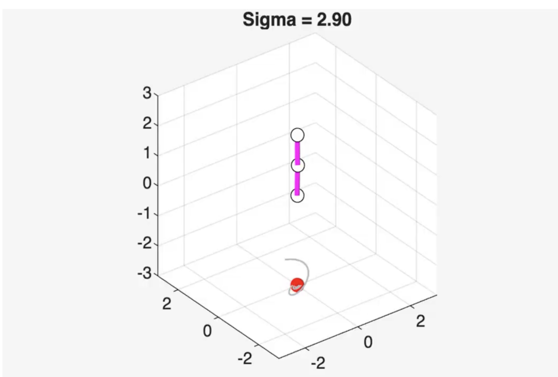

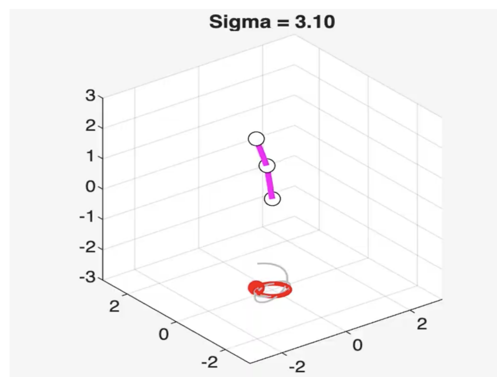

The white dots(Beads – Base, Bead 1, Bead 2) and magenta links represent the 2 link model of the cilia. The gray and red trails trace out the (x,y) positions of where Bead 2 has been, with the red trail being the more recent positions. The red dot is the current (x,y) position of the Bead 2.

5 The N-link Model

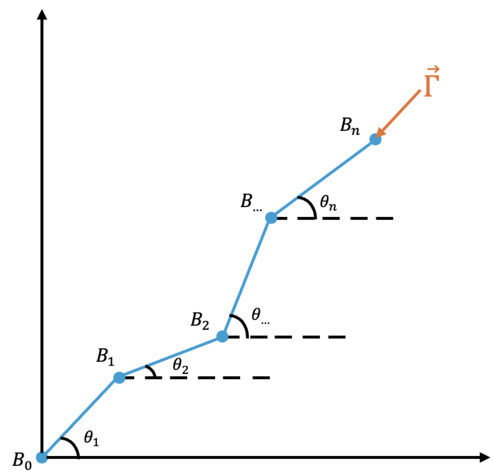

Figure 8: N-link model

Another generalization of the two-link model is the N-link model, where we once again consider a discrete filament, but now with N beads instead of just two. In the following section, we outline the derivation of the N-link model, as well as conduct a bifurcation analysis, where the parameters are the number of beads, N, and the non-dimensional forcing amount, Σ.

5.1 Derivation of the N-link Model

The first thing we must do is re-assess how we define the position vector for each bead. In general, the position vector for the jth bead is given by

$$\vec{r}_j = l\left(\sum_{i=1}^{j}\cos(\theta_i), \sum_{i=1}^{j}\sin(\theta_i)\right).$$

Differentiating, we can derive both the velocity of the jth bead, $\vec{v}_j$ as well as the variation, $\delta\vec{r}_j$:

$$\begin{aligned}
\boldsymbol{v_j} &= l\left(-\sum_{i=1}^{j}\dot{\theta}_i\sin\theta_i, \sum_{i=1}^{j}\dot{\theta}_i\cos\theta_i\right) \\
&= l\sum_{i=1}^{j}\dot{\theta}_i(-\sin\theta_i, \cos\theta_i) \\
\implies \delta\boldsymbol{r_j} &= l\sum_{i=1}^{j}\delta\theta_i(-\sin\theta_i, \cos\theta_i).
\end{aligned}$$

Now, we redefine the forces acting on the beads:

$\underline{\boldsymbol{\Gamma}}$:

$$\boldsymbol{\Gamma} = \Gamma\hat{\boldsymbol{t}} = \Gamma(\cos\theta_N, \sin\theta_N)$$

$\underline{\boldsymbol{F_{drag_j}}}$:

$$\boldsymbol{F_{drag_j}} = -\zeta\boldsymbol{v_j}, \quad j = 1, 2, \dots, N$$

$\underline{\boldsymbol{F_{spr_j}}:}$

$$\begin{aligned}\boldsymbol{F_{spr_1}} &= -k\theta_1 \\ \boldsymbol{F_{spr_j}} &= -k(\theta_j - \theta_{j-1}), \quad j = 2, \dots, N\end{aligned}$$

Thus, the virtual work equation then becomes

$$\boldsymbol{\Gamma\delta r_N} + \sum_{j=1}^{N} \boldsymbol{F_{drag_j}\delta r_j} + \boldsymbol{F_{spr_1}\delta r_1} + \sum_{j=2}^{N} \boldsymbol{F_{spr_j}\delta r_j}$$

We must now expand each of these terms in order to write the virtual work for each individual bead as $c_j\delta\theta_j = 0$; just as with the two-link model, we will use the arbitrariness of $\delta\theta_j$ to claim $c_j = 0$, thereby allowing us to derive a system of ODEs for the motion of the filament. We start with the work done by the tangential force:

$$\begin{aligned}\boldsymbol{\Gamma\delta r_N} &= -\Gamma(\cos\theta_N, \sin\theta_N) \cdot \ell \left[\sum_{i=1}^{N} \delta\theta_i(-\sin\theta_i, \cos\theta_i)\right] \\ &= -\Gamma\ell \left[\sum_{i=1}^{N} \delta\theta_i \left(-\sin\theta_i \cos\theta_N + \sin\theta_N \cos\theta_i\right)\right] \\ &= -\Gamma\ell \left[\sum_{i=1}^{N} \delta\theta_i \sin(\theta_N - \theta_i)\right] \\ &= \sum_{i=1}^{N} \delta\theta_i \left[\Gamma\ell \sin(\theta_i - \theta_N)\right].\end{aligned}$$

We verify this is accurate for $N = 2$:

$$\begin{aligned}\sum_{i=1}^{2} \delta\theta_i \left[\Gamma\ell \sin(\theta_i - \theta_2)\right] &= \delta\theta_1 \left[\Gamma\ell \sin(\theta_1 - \theta_2)\right] + \delta\theta_2 \left[\Gamma\ell \sin(\theta_2 - \theta_2)\right] \\ &= \delta\theta_1 \left[\Gamma\ell \sin(\theta_1 - \theta_2)\right] + \delta\theta_2 \left[\Gamma\ell \sin(0)\right] \\ &= \delta\theta_1 \left[\Gamma\ell \sin(\theta_1 - \theta_2)\right].\end{aligned}$$

Now, we repeat the process for the virtual work done by the fluid drag forces:

$$\begin{aligned}\sum_{j=1}^{N} \boldsymbol{F}_{drag_j} \cdot \boldsymbol{\delta r}_j &= \sum_{j=1}^{N} -\zeta \boldsymbol{v}_j \cdot \boldsymbol{\delta r}_j \\ &= -\zeta\ell^2 \sum_{j=1}^{N} \left(\sum_{k=1}^{j} \dot{\theta}_k(-\sin\theta_k, \cos\theta_k) \cdot \sum_{i=1}^{j} \delta\theta_i(-\sin\theta_i, \cos\theta_i)\right) \\ &= -\zeta\ell^2 \sum_{j=1}^{N} \Big[\dot{\theta}_1\delta\theta_1(\sin^2\theta_1 + \cos^2\theta_1) + \dot{\theta}_1\delta\theta_2(\sin\theta_1 \sin\theta_2 + \cos\theta_1 \cos\theta_2) + \cdots \\ &\qquad + \dot{\theta}_k\delta\theta_i(\sin\theta_k \sin\theta_i + \cos\theta_k \cos\theta_i) + \cdots\Big] \\ &= -\zeta\ell^2 \sum_{j=1}^{N} \sum_{k=1}^{j} \sum_{i=1}^{j} \dot{\theta}_k \delta\theta_i \cos(\theta_i - \theta_k).\end{aligned}$$

Checking for $N = 2$ again:

$$(j = 1) \quad \sum_{k=1}^{1}\sum_{i=1}^{1} \delta\theta_i \left[-\zeta\ell^2\dot{\theta}_k\cos(\theta_k - \theta_i)\right] = \delta\theta_1 \left[-\zeta\ell^2\dot{\theta}_1\cos(\theta_1 - \theta_1)\right]$$
$$= \delta\theta_1 \left[-\zeta\ell^2\dot{\theta}_1\right].$$

$$\begin{aligned}(j = 2) \quad \sum_{k=1}^{2}\sum_{i=1}^{2} \delta\theta_i \left[-\zeta\ell^2\dot{\theta}_k\cos(\theta_k - \theta_i)\right] &= \delta\theta_1 \left[-\zeta\ell^2\dot{\theta}_1\cos(\theta_1 - \theta_1)\right] \\
&+ \delta\theta_2 \left[-\zeta\ell^2\dot{\theta}_1\cos(\theta_1 - \theta_2)\right] \\
&+ \delta\theta_1 \left[-\zeta\ell^2\dot{\theta}_2\cos(\theta_2 - \theta_1)\right] \\
&+ \delta\theta_2 \left[-\zeta\ell^2\dot{\theta}_2\cos(\theta_2 - \theta_2)\right] \\
&= \delta\theta_1 \left[-\zeta\ell^2\left(\dot{\theta}_1 + \dot{\theta}_2\cos(\theta_2 - \theta_1)\right)\right] \\
&+ \delta\theta_2 \left[-\zeta\ell^2\left(\dot{\theta}_1\cos(\theta_1 - \theta_2) + \dot{\theta}_2\right)\right].\end{aligned}$$

Now, still working with the virtual work done by the fluid drag forces, we extend to $N = 3$, as there is an interesting pattern that appears (note that for $j = 1, 2$, we get the same result as before, so we only expand for $j = 3$ here):

$$\begin{aligned}\sum_{k=1}^{3}\sum_{i=1}^{3} \delta\theta_i \left[-\zeta\ell^2\dot{\theta}_k\cos(\theta_k - \theta_i)\right] &= \delta\theta_1 \left[-\zeta\ell^2\dot{\theta}_1\cos(\theta_1 - \theta_1)\right] \\
&+ \delta\theta_2 \left[-\zeta\ell^2\dot{\theta}_1\cos(\theta_1 - \theta_2)\right] \\
&+ \delta\theta_3 \left[-\zeta\ell^2\dot{\theta}_1\cos(\theta_1 - \theta_3)\right] \\
&+ \delta\theta_1 \left[-\zeta\ell^2\dot{\theta}_2\cos(\theta_2 - \theta_1)\right] \\
&+ \delta\theta_2 \left[-\zeta\ell^2\dot{\theta}_2\cos(\theta_2 - \theta_2)\right] \\
&+ \delta\theta_3 \left[-\zeta\ell^2\dot{\theta}_2\cos(\theta_2 - \theta_3)\right] \\
&+ \delta\theta_1 \left[-\zeta\ell^2\dot{\theta}_3\cos(\theta_3 - \theta_1)\right] \\
&+ \delta\theta_2 \left[-\zeta\ell^2\dot{\theta}_3\cos(\theta_3 - \theta_2)\right] \\
&+ \delta\theta_3 \left[-\zeta\ell^2\dot{\theta}_3\cos(\theta_3 - \theta_3)\right].\end{aligned}$$

Now, we gather all the terms for $j = 1, 2, 3$ in terms of $\delta\theta_j$:

$$
\begin{aligned}
&\delta\theta_1 \left[-\zeta\ell^2 \left(3\dot\theta_1 + 2\dot\theta_2 \cos(\theta_1-\theta_2) + \dot\theta_3 \cos(\theta_1-\theta_3) \right) \right] \\
&\quad + \delta\theta_2 \left[-\zeta\ell^2 \left(2\dot\theta_1 \cos(\theta_1-\theta_2) + 2\dot\theta_2 + \dot\theta_3 \cos(\theta_2-\theta_3) \right) \right] \\
&\quad + \delta\theta_3 \left[-\zeta\ell^2 \left(\dot\theta_1 \cos(\theta_1-\theta_3) + \dot\theta_2 \cos(\theta_2-\theta_3) + \dot\theta_3 \right) \right].
\end{aligned}
$$

Note that there appears to be a pattern for the coefficients for each $\dot\theta$, which can be summarized in the following symmetric matrix:

$$
J_3 = \begin{bmatrix} 3 & 2 & 1 \\ 2 & 2 & 1 \\ 1 & 1 & 1 \end{bmatrix}.
$$

Repeating for higher values of N reveals the following generalized version of the above matrix:

$$
J_N = \begin{bmatrix} N & N-1 & N-2 & \dots & 1 \\ N-1 & N-1 & N-2 & \dots & 1 \\ N-2 & N-2 & N-2 & \dots & 1 \\ \vdots & \vdots & \vdots & \vdots & \vdots \\ 1 & 1 & 1 & \dots & 1 \end{bmatrix}.
$$

This matrix will come in handy later, when we derive full equations of motion.

Now, we move onto the work done by the torsional spring force:

$$
\boldsymbol{F}_{\mathrm{spr},1}\, \delta\theta_1 = (-k\theta_1)\delta\theta_1.
$$

$$
\begin{aligned}
\sum_{j=1}^{N} \boldsymbol{F}_{\mathrm{spr},j} \left(\delta\theta_j - \delta\theta_{j-1} \right) &= -k \left(\theta_1\delta\theta_1 + \sum_{j=2}^{N} \left(\delta\theta_j - \delta\theta_{j-1} \right) \left(\theta_j - \theta_{j-1} \right) \right) \\
&= -k\theta_1\delta\theta_1 + \sum_{j=2}^{N} \left(\delta\theta_{j-1} \left[k(\theta_j-\theta_{j-1}) \right] + \delta\theta_j \left[k(\theta_{j-1}-\theta_j) \right] \right) \\
&= \delta\theta_1 \left[k(\theta_2 - 2\theta_1) \right] + \delta\theta_2\, \underbrace{k([k(\theta_1-\theta_2) + k(\theta_3-\theta_2)]}_{\theta_1-2\theta_2+\theta_3)} \\
&\quad + \dots + \delta\theta_{N-1} \underbrace{\left[k(\theta_N-\theta_{N-1}) + k(\theta_{N-2}-\theta_{N-1}) \right]}_{k(\theta_{N-2}-2\theta_{N-1}+\theta_N)} \\
&\quad + \delta\theta_N \left[k(\theta_{N-1}-\theta_N) \right].
\end{aligned}
$$

Returning to the virtual work equation, we now see a sum in the form of:

$$
\sum_{i=1}^{N} C_i \delta\theta_i = 0.
$$

Since the $\delta\theta_i$ are arbitrary, we must have

$$
C_i = 0, \qquad i = 1, \dots, N.
$$

Returning to the virtual work expression, and non-dimensionalizing in the same manner as we did in section 2, we end up with the following ODE:

$$\boxed{\Sigma\sin(\theta_i-\theta_N)-\sum_{k=1}^{N}D_{ik}\dot{\theta}_k\cos(\theta_k-\theta_i)+\Phi_i=0,\qquad i=1,2,\ldots,N,\qquad \theta_0=0}$$

Here,

$$D=\begin{bmatrix} N & N-1 & N-2 & \cdots & 1\\ N-1 & N-1 & N-2 & \cdots & 1\\ N-2 & N-2 & N-2 & \cdots & 1\\ \vdots & \vdots & \vdots & \ddots & \vdots\\ 1 & 1 & 1 & \cdots & 1\end{bmatrix},$$

and

$$\Phi_i=\begin{cases}-2\theta_1+\theta_2, & i=1,\\ \theta_{i-1}-2\theta_i+\theta_{i+1}, & i\in(1,N),\\ \theta_{N-1}-\theta_N, & i=N.\end{cases}$$

5.2 Bifurcation Analysis

In order to conduct a bifurcation analysis, we must re-frame the equations of motion as the system $\boldsymbol{\theta'}=M^{-1}\boldsymbol{b}=\boldsymbol{f}(\boldsymbol{\theta},\Sigma,N)$ and then compute the Jacobian of $\boldsymbol{f}$; Hopf bifurcations occur where the real components of the maximum eigenvalues of this Jacobian cross the zero-axis in the parameter space of Σ and N. We can re-frame our problem as follows:

$$\Sigma\sin(\theta_i-\theta_N)-\sum_{k=1}^{N}D_{ik}\dot{\theta}_k\cos(\theta_k-\theta_i)+\Phi_i=0$$

$$\sum_{k=1}^{N}D_{ik}\dot{\theta}_k\cos(\theta_k-\theta_i)=\Sigma\sin(\theta_i-\theta_N)+\Phi_i$$

Now expanding this into matrix form for each i:

$$\begin{bmatrix}\sum_{k=1}^{N}D_{1k}\dot{\theta}_k\cos(\theta_k-\theta_1)\\ \sum_{k=1}^{N}D_{2k}\dot{\theta}_k\cos(\theta_k-\theta_2)\\ \vdots\\ \sum_{k=1}^{N}D_{Nk}\dot{\theta}_k\cos(\theta_k-\theta_N)\end{bmatrix}=\begin{bmatrix}\Sigma\sin(\theta_1-\theta_N)-2\theta_1+\theta_2\\ \vdots\\ \Sigma\sin(\theta_{N-1}-\theta_N)+\theta_{N-2}-2\theta_{N-1}+\theta_N\\ \theta_{N-1}-\theta_N\end{bmatrix}$$

$$\begin{bmatrix}D_{11}\dot{\theta}_1+D_{12}\dot{\theta}_2\cos(\theta_1-\theta_2)+\ldots+D_{N1}\dot{\theta}_N\cos(\theta_1-\theta_N)\\ D_{21}\dot{\theta}_1\cos(\theta_1-\theta_2)+D_{22}\dot{\theta}_2+\ldots+D_{N2}\dot{\theta}_N\cos(\theta_2-\theta_N)\\ \vdots\\ D_{N1}\dot{\theta}_1\cos(\theta_1-\theta_N)+D_{N2}\dot{\theta}_2\cos(\theta_2-\theta_N)+\ldots+D_{NN}\dot{\theta}_N\end{bmatrix}=\begin{bmatrix}\Sigma\sin(\theta_1-\theta_N)-2\theta_1+\theta_2\\ \vdots\\ \Sigma\sin(\theta_{N-1}-\theta_N)+\theta_{N-2}-2\theta_{N-1}+\theta_N\\ \theta_{N-1}-\theta_N\end{bmatrix}$$

$$\underbrace{\begin{bmatrix}D_{11} & D_{12}\cos(\theta_1-\theta_2) & \ldots & D_{1N}\cos(\theta_1-\theta_N)\\ D_{21}\cos(\theta_1-\theta_2) & D_{12} & \ldots & D_{2N}\cos(\theta_2-\theta_N)\\ \vdots & \vdots & \ddots & \vdots\\ D_{N1}\cos(\theta_1-\theta_N) & D_{N2}\cos(\theta_2-\theta_N) & \ldots & D_{NN}\end{bmatrix}}_{M}\underbrace{\begin{bmatrix}\theta_1'\\ \theta_2'\\ \vdots\\ \theta_N'\end{bmatrix}}_{\boldsymbol{\theta'}}=\underbrace{\begin{bmatrix}\Sigma\sin(\theta_1-\theta_N)-2\theta_1+\theta_2\\ \vdots\\ \Sigma\sin(\theta_{N-1}-\theta_N)+\theta_{N-2}-2\theta_{N-1}+\theta_N\\ \theta_{N-1}-\theta_N\end{bmatrix}}_{\boldsymbol{b}}$$

$$\implies\boldsymbol{\theta'}=M^{-1}\boldsymbol{b}=\boldsymbol{f}(\boldsymbol{\theta};\Sigma;N)$$

Note that $\boldsymbol{\theta}_* \equiv 0$ is a valid critical point of this system, and therefore we can linearize around it; in other words, we evaluate our Jacobian at this $\boldsymbol{\theta}_*$ and then conduct our previously outlined eigenvalue analysis to determine where the Hopf bifurcation is. Mathematically, we find the eigenvalues (which are functions of Σ and N) of:

$$J_{\boldsymbol{f}}\big|_{\boldsymbol{\theta}=\boldsymbol{\theta}_*} = \nabla_{\boldsymbol{\theta}} \boldsymbol{f}(\boldsymbol{\theta}; \Sigma; N)\big|_{\boldsymbol{\theta}=\boldsymbol{\theta}_*}$$

We used MATLAB to sweep over a spectrum of Σ and N values to determine where the real components of the eigenvalues of $J_{\boldsymbol{f}}$ cross the zero-axis. We found that while the two-link model has a single Hopf bifurcation at $\Sigma = 3$, the N-link model's bifurcation point changes with the number of beads, N. Specifically, the critical tangential forcing amount *decreases* as N increases.

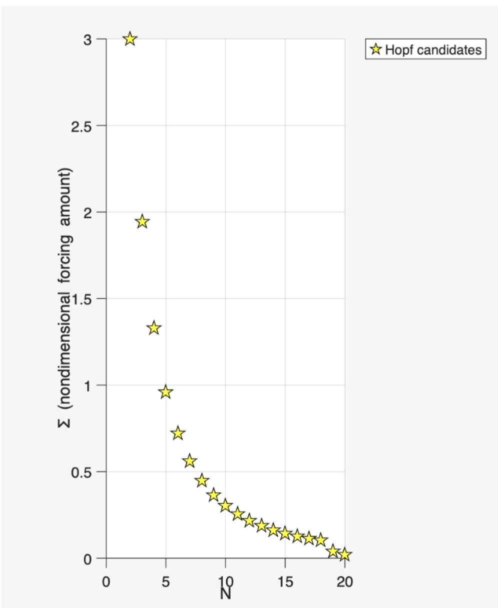

(a) N-link bifurcation diagram

N	Critical Forcing Amount
2	3
3	1.9431
4	1.3302
5	0.95869
6	0.72057
7	0.55958
8	0.44631
9	0.36395
10	0.30318
11	0.25419
12	0.21716
13	0.18552
14	0.1627
15	0.14166
16	0.12462
17	0.11147
18	0.10233
19	0.037702
20	0.019124

(b) N-link bifurcation table

Figure 9: Hopf bifurcation locations

Figure 10 gives an example of a Hopf bifurcation for $N = 3$:

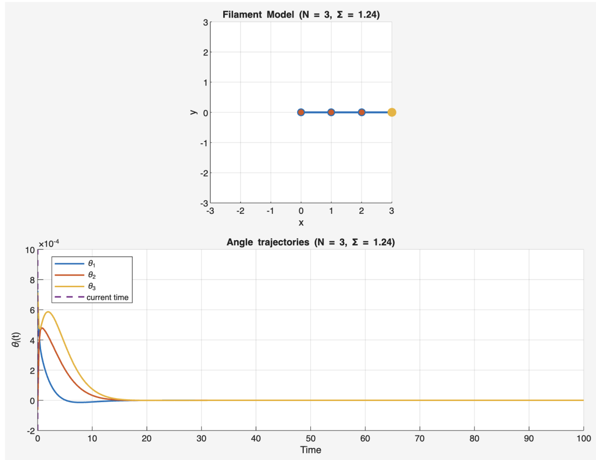

(a) $N = 3$, $\Sigma = 1.24$

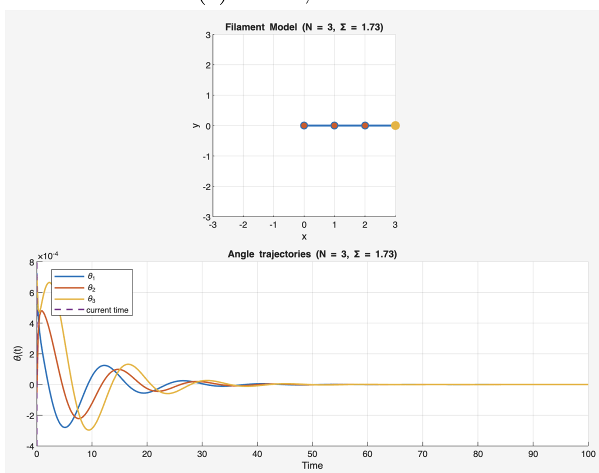

(b) $N = 3$, $\Sigma = 1.73$

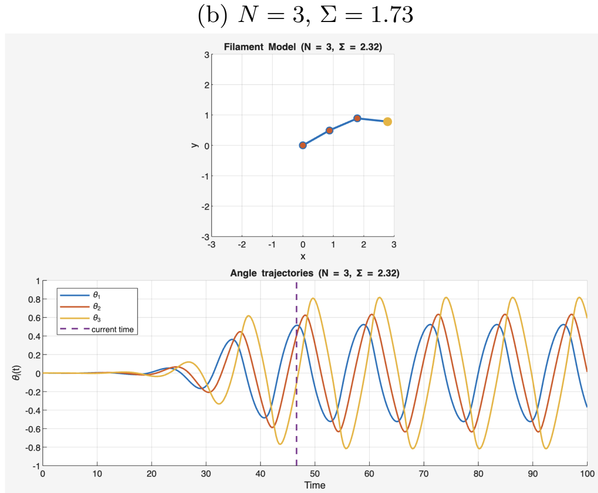

(c) $N = 3$, $\Sigma = 2.32$

Figure 10: Hopf bifurcation locations

6 Extension to N-Cilia with Hydrodynamic Coupling

6.1 Virtual Work Done by Fluid Drag Forces with Hydrodynamic Coupling

6.1.1 Force Derivation

Previously, we only considered local hydrodynamic forces, i.e. the fluid drag force exerted on B did not affect A. In matrix notation, we can view this as follows:

$$\begin{pmatrix} \boldsymbol{F_A} \\ \boldsymbol{F_B} \end{pmatrix} = -\begin{pmatrix} \zeta I & 0 \\ 0 & \zeta I \end{pmatrix} \begin{pmatrix} \boldsymbol{v_A} \\ \boldsymbol{v_B} \end{pmatrix}.$$

However, when considering hydrodynamic coupling, we replace the above formulation with the following:

$$\boldsymbol{v} = -\mathbf{M}\mathbf{F}_{\boldsymbol{drag}}.$$

where $\boldsymbol{v}$ is a vector containing the velocities, $\mathbf{M}$ is the mobility matrix obtained by the regularized Stokeslet method of images on a no-slip wall [1], and $\mathbf{F}_{\boldsymbol{drag}}$ is the vector of fluid drag forces on each bead. It then follows that we can solve for the fluid drag force by writing

$$\mathbf{F}_{\boldsymbol{drag}} = -\mathbf{M}^{-1}\boldsymbol{v}.$$

Now recall from the two-link model that we were able to write the velocities as $\boldsymbol{v_A} = \dot{\theta}_1 l(-\sin\theta_1, \cos\theta_1)$ and $\boldsymbol{v_B} = l[\dot{\theta}_1(-\sin\theta_1, \cos\theta_1) + \dot{\theta}_2(-\sin\theta_2, \cos\theta_2)]$. We can write this in vector notation as follows:

$$\begin{aligned} \boldsymbol{v} &= \begin{pmatrix} \dot{\theta}_1 l(-\sin\theta_1, \cos\theta_1) \\ \dot{\theta}_1 l(-\sin\theta_1, \cos\theta_1) + \dot{\theta}_2 l(-\sin\theta_2, \cos\theta_2) \end{pmatrix} \\ &= l \underbrace{\begin{pmatrix} (-\sin\theta_1, \cos\theta_1) & 0 \\ (-\sin\theta_1, \cos\theta_1) & (-\sin\theta_2, \cos\theta_2) \end{pmatrix}}_{\tilde{Q}(\boldsymbol{\theta})} \cdot \begin{pmatrix} \dot{\theta}_1 \\ \dot{\theta}_2 \end{pmatrix} \\ &= l\tilde{Q}(\boldsymbol{\theta}) \cdot \dot{\boldsymbol{\theta}}. \end{aligned}$$

Now that we have rephrased the velocity more compactly in vector notation, we can easily generalize it to n-cilia rather than a single cilium. To do this, we rewrite $\boldsymbol{\theta}$ to be a stacked vector containing all angles in a system of n-cilia:

$$\boldsymbol{\theta} = \begin{pmatrix} \boldsymbol{\theta}_1 \\ \vdots \\ \boldsymbol{\theta}_n \end{pmatrix} = \begin{pmatrix} \theta_{1,1} \\ \theta_{1,2} \\ \vdots \\ \theta_{n,1} \\ \theta_{n,2} \end{pmatrix}.$$

We then use $\tilde{Q}(\boldsymbol{\theta}_i)$ (where $\boldsymbol{\theta}_i = \begin{pmatrix} \theta_{i,1} & \theta_{i,2} \end{pmatrix}^\top$) to form

$$Q(\boldsymbol{\theta}) = \begin{pmatrix} \tilde{Q}(\boldsymbol{\theta}_1) & 0 & \dots & 0 \\ 0 & \tilde{Q}(\boldsymbol{\theta}_2) & \dots & 0 \\ \vdots & & \ddots & 0 \\ 0 & \dots & & \tilde{Q}(\boldsymbol{\theta}_n) \end{pmatrix}.$$

Thus, the drag for every bead in our n-cilia system can be written as

$$\mathbf{F}_{drag} = -l\mathrm{M}^{-1}Q(\boldsymbol{\theta})\dot{\boldsymbol{\theta}}$$

6.1.2 Virtual Work Derivation

To see how much the drag force contributes to the virtual work equation, we can take its dot-product with the stacked vector $\delta\boldsymbol{r} = \begin{pmatrix}\delta r_{1,1} & \delta r_{1,2} & \dots & \delta r_{n,1} & \delta r_{n,2}\end{pmatrix}^\top$. This vector evaluates to something very similar to $\boldsymbol{v}$, which we just calculated, but with $\delta\theta$ rather than $\dot{\theta}$. Thus, we get

$$\delta\boldsymbol{r} = lQ(\boldsymbol{\theta})\delta\boldsymbol{\theta}$$

and the contribution of drag to the virtual work equation is

$$\begin{aligned}\mathbf{F}_{drag} \cdot \delta\boldsymbol{r} &= \mathbf{F}_{drag}^\top \delta\boldsymbol{r} \\ &= \delta\boldsymbol{r}^\top \mathbf{F}_{drag} \\ &= \delta\boldsymbol{\theta}^\top \left(-l^2 Q(\boldsymbol{\theta})^\top \mathrm{M}^{-1} Q(\boldsymbol{\theta})\dot{\boldsymbol{\theta}}\right).\end{aligned}$$

6.2 Virtual Work Done by Torsional Spring Forces

6.2.1 Force Derivation

The next forces we will extend to n-cilia are the torsional spring forces. Recall from two-link model that the spring forces were $F_{spr_O} = -k\theta_1$ and $F_{spr_A} = -k(\theta_2 - \theta_1)$. We can express this in matrix/vector notation as

$$\begin{aligned}\mathbf{F}_{spr} &= -k \begin{pmatrix}\theta_1 \\ \theta_2 - \theta_1\end{pmatrix} \\ &= -k \underbrace{\begin{pmatrix}1 & 0 \\ -1 & 1\end{pmatrix}}_{\tilde{L}} \begin{pmatrix}\theta_1 \\ \theta_2\end{pmatrix} \\ &= -k\tilde{L}\boldsymbol{\theta}.\end{aligned}$$

We can easily extend this to n-cilia similarly to how we did with the drag forces: rewrite $\boldsymbol{\theta}$ to be a stacked vector of all θ's in the entire system and write L to be

$$L = \begin{pmatrix}\tilde{L} & 0 & \dots & 0 \\ 0 & \tilde{L} & \dots & 0 \\ \vdots & & \ddots & 0 \\ 0 & \dots & & \tilde{L}\end{pmatrix}.$$

Then for our full n-cilia system we have:

$$\mathbf{F}_{spr} = -kL\boldsymbol{\theta}.$$

6.2.2 Virtual Work Derivation

Now, we can see how much virtual work is being done by the spring forces. In the two-link model, we saw that the contribution of the spring forces were $(F_{spr_O} - F_{spr_A})\delta\theta_1 + F_{spr_A}\delta\theta_2$. Expressing this in matrix/vector notation:

$$
\begin{aligned}
\mathbf{F}_{spr} \cdot \delta\boldsymbol{\theta} &= \begin{pmatrix} F_{spr_O} - F_{spr_A} \\ F_{spr_A} \end{pmatrix} \cdot \begin{pmatrix} \delta\theta_1 \\ \delta\theta_2 \end{pmatrix} \\
&= \underbrace{\begin{pmatrix} 1 & -1 \\ 0 & 1 \end{pmatrix}}_{\tilde{L}^\top} \begin{pmatrix} F_{spr_O} \\ F_{spr_A} \end{pmatrix} \cdot \begin{pmatrix} \delta\theta_1 \\ \delta\theta_2 \end{pmatrix}
\end{aligned}
$$

Now, substituting in our derivation for $\mathbf{F}_{spr}$: and generalizing to n-cilia:

$$
\begin{aligned}
\mathbf{F}_{spr} \cdot \delta\boldsymbol{\theta} &= \mathbf{F}_{spr}^\top \delta\boldsymbol{\theta} \\
&= \delta\boldsymbol{\theta}^\top \mathbf{F}_{spr} \\
&= \delta\boldsymbol{\theta}^\top \left[-kL^\top L\boldsymbol{\theta} \right]
\end{aligned}
$$

6.3 Re-deriving the Follower Force

6.3.1 Virtual Work Derivation

Since the follower force is much simpler in comparison to the other forces (it only acts at ends of the cilia), we can jump straight into the virtual work contribution. In the two-link model, we derived that for a single cilia the virtual work done by the follower force was $\boldsymbol{\Gamma}\delta r_B = (\Gamma l \sin(\theta_1 - \theta_2))\delta\theta_1$. Expressing this in matrix/vector notation:

$$
\boldsymbol{\Gamma}\delta r_B = \Gamma l \begin{pmatrix} \sin(\theta_1 - \theta_2) \\ 0 \end{pmatrix} \cdot \begin{pmatrix} \delta\theta_1 \\ \delta\theta_2 \end{pmatrix}
$$

Extending this to n-cilia is once again straightforward:

$$
\begin{aligned}
\boldsymbol{\Gamma}\delta\boldsymbol{r} &= \Gamma l \underbrace{\begin{pmatrix} \sin(\theta_{1,1} - \theta_{1,2}) \\ 0 \\ \sin(\theta_{2,1} - \theta_{2,2}) \\ 0 \\ \vdots \\ \sin(\theta_{n-1,1} - \theta_{n-1,2}) \\ 0 \\ \sin(\theta_{n,1} - \theta_{n,2}) \\ 0 \end{pmatrix}}_{N(\boldsymbol{\theta})} \cdot \begin{pmatrix} \delta\theta_{1,1} \\ \delta\theta_{1,2} \\ \delta\theta_{2,1} \\ \delta\theta_{2,2} \\ \vdots \\ \delta\theta_{n-1,1} \\ \delta\theta_{n-1,2} \\ \delta\theta_{n,1} \\ \delta\theta_{n,2} \end{pmatrix} \\
&= [\Gamma l N(\boldsymbol{\theta})] \cdot \delta\boldsymbol{\theta} \\
&= \delta\boldsymbol{\theta}^\top [\Gamma l N(\boldsymbol{\theta})]
\end{aligned}
$$

6.4 Equations of Motion

Now that we have the contributions of the each of the forces to virtual work, we can set them all equal to the zero-vector $\mathbf{0}$:

$$
\begin{aligned}
&\delta\boldsymbol{\theta}^\top \left[-l^2 Q(\boldsymbol{\theta})^\top \mathrm{M}^{-1} Q(\boldsymbol{\theta})\dot{\boldsymbol{\theta}} \right] + \delta\boldsymbol{\theta}^\top \left[-kL^\top L\boldsymbol{\theta} \right] + \delta\boldsymbol{\theta}^\top [\Gamma l N(\boldsymbol{\theta})] = \mathbf{0} \\
\iff\ & \delta\boldsymbol{\theta}^\top \left[-l^2 Q(\boldsymbol{\theta})^\top \mathrm{M}^{-1} Q(\boldsymbol{\theta})\dot{\boldsymbol{\theta}} - kL^\top L\boldsymbol{\theta} + \Gamma l N(\boldsymbol{\theta}) \right] = \mathbf{0}
\end{aligned}
$$

So, the final dimensional equation of motion is:

$$\Gamma l N(\boldsymbol{\theta}) - l^2 Q(\boldsymbol{\theta})^\top \mathrm{M}^{-1} Q(\boldsymbol{\theta})\dot{\boldsymbol{\theta}} - kL^\top L\boldsymbol{\theta} = \mathbf{0}.$$

7 Conclusion

Inspired by De Canio et al's 2-Link Model [3], our team came up with four models to explain cilia beats on the local and global scale. Our team first re-derived the 2-Link Model and conducted bifurcation analysis to confirm that this model reproduces the flapping motions of individual cilium by exhibiting a Hopf bifurcation point at $\Sigma = 3$. Motivated by studies on the internal structures of cilia and dynein motors [5], we proposed a 2-Link Coupled Follower Model where two equal and opposite follower forces act upon two connected filaments. Despite exhibiting oscillatory behaviors, this model fails to replicate the Hopf bifurcations characteristic of the 2-Link Model. We generalized the 2-Link Model by considering a three dimensional follower force and N-Links. The N-Link Model shows Hopf bifurcations, similar to the 2-Link Model. One major finding is that the critical follower force Γ decreases as the number of beads increases. Noting that cilia carpet exhibit spontaneous metachronal coordination, we tried to derive an equation of motion for multiple 2-Link Models coupled by nonlocal fluid forces. These forces are modeled by the dimensionless Stokes equation in the low Reynolds number regime.

This paper focuses on the derivation of these four models. It is a first step towards understanding the spontaneous beating of a cilium as well as cilia carpets. More in depth stability analysis is required to extract insights about the mechanism of cilia motion. The models also need to be tweaked and simplifications should be relaxed, especially for the 2-Link Coupled Follower Model, in order to better recapitulate real life cilia.

References

[1] Josephine Ainley et al. "The method of images for regularized Stokeslets". In: *Journal of Computational Physics* 227.9 (2008), pp. 4600–4616. ISSN: 0021-9991. DOI: https://doi.org/10.1016/j.jcp.2008.01.032. URL: https://www.sciencedirect.com/science/article/pii/S0021999108000417.

[2] John Blake. "Fluid Mechanics of Ciliary Propulsion". In: *Computational Modeling in Biological Fluid Dynamics*. Ed. by Lisa J. Fauci and Shay Gueron. New York, NY: Springer New York, 2001, pp. 1–51. ISBN: 978-1-4613-0151-6.

[3] Gabriele De Canio, Eric Lauga, and Raymond E. Goldstein. "Spontaneous oscillations of elastic filaments induced by molecular motors". In: *Journal of The Royal Society Interface* 14.136 (Nov. 30, 2017), p. 20170491. ISSN: 1742-5689, 1742-5662. DOI: 10.1098/rsif.2017.0491. URL: https://royalsocietypublishing.org/rsif/article/14/136/20170491/64852/Spontaneous-oscillations-of-elastic-filaments (visited on 04/02/2026).

[4] Natan Osterman and Andrej Vilfan. "Finding the ciliary beating pattern with optimal efficiency". In: *Proceedings of the National Academy of Sciences* 108.38 (2011), pp. 15727–15732. DOI: 10.1073/pnas.1107889108. eprint: https://www.pnas.org/doi/pdf/10.1073/pnas.1107889108. URL: https://www.pnas.org/doi/abs/10.1073/pnas.1107889108.

[5] P. Satir. "Structural basis of ciliary movement". In: *Environmental Health Perspectives* 35 (Apr. 1980), pp. 77–82. DOI: 10.1289/ehp.803577.